NUMERICAL ANALYSIS TO OPTIMIZE THE HEAT TRANSFER RATE OF TUBE-IN-TUBE HELICAL COIL HEAT EXCHANGER

A REPORT SUBMITTED IN PARTIAL FULFILMENT
OF THE REQUIREMENTS FOR THE DEGREE OF

Master of Technology
in
Mechanical Engineering

By

SATYABRATA KANUNGO

(212ME3312)

Department of Mechanical Engineering
National Institute Of Technology Rourkela
Rourkela-769008, Odisha

2014

NUMERICAL ANALYSIS TO OPTIMIZE THE HEAT TRANSFER RATE OF TUBE-IN-TUBE HELICAL COIL HEAT EXCHANGER

A REPORT SUBMITTED IN PARTIAL FULFILMENT

OF THE REQUIREMENTS FOR THE DEGREE OF

Master of Technology

in

Mechanical Engineering

By

SATYABRATA KANUNGO

(212ME3312)

Under the supervision of

Prof. A.K. Satapathy

Department of Mechanical Engineering

National Institute Of Technology Rourkela

Rourkela-769008, Odisha

2014

National Institute of Technology

Rourkela

CERTIFICATE

This is to certify that the thesis entitled, "**NUMERICAL ANALYSIS TO OPTIMIZE THE HEAT TRANSFER RATE OF TUBE-IN-TUBE HELICAL COIL HEAT EXCHANGER**" submitted by Mr. **SATYABRATA KANUNGO** in partial fulfillment of the requirements for the award of Master of Technology Degree in Mechanical Engineering with specialization in Thermal Engineering at the National Institute of Technology, Rourkela (Deemed University) is an authentic work carried out by him under my supervision and guidance.

To the best of my knowledge, the matter embodied in the thesis has not been submitted to any other University/ Institute for the award of any degree or diploma.

Date:

Prof. A. K. Satapathy

Dept. of Mechanical Engineering

National Institute of Technology Rourkela

Rourkela-769008

ACKNOWLEDGEMENT

I express my deep sense of gratitude and indebtedness to my project supervisor Prof. A.K. Satapathy, Professor, Department of Mechanical Engineering for providing precious guidance, inspiring discussions and constant supervision throughout the course of this work.

I am grateful to Prof. K.P Maity, Head of the Department of Mechanical Engineering for providing me the necessary facilities in the department. I am also thankful to all the staff members of the department of Mechanical Engineering and to all my well wishers for their inspiration and help. I would also like to thank Mr. Sagar Das (BTECH 4th year) and Miss. Laxmi Priya Sahoo (BTECH 4th year) mechanical students who helped me in completion of my project.

I feel pleased and privileged to full fill my parent's ambition and I am greatly indebted to them for bearing the inconvenience during my M Tech. course.

Date:

Place:

Satyabrata kanungo

Roll.no-212ME3312

ABSTRACT

Working towards the goal of saving energies and to make compact the design for mechanical and chemical devices and plants, the enhancement of heat transfer is one of the key factors in design of heat exchangers. In this process without application of external power we can enhance the heat transfer rate by modifying the design by providing the helical tubes, extended surface or swirl flow devices. Helical tube heat exchanger finds applications in automobile, aerospace, power plant and food industries due to certain advantage such as compact structure, larger heat transfer surface area and improved heat transfer capability. In this paper numerical study of helical coil tube-in-tube heat exchanger is done for different boundary conditions and optimizes condition of heat transfer is found out for different D/d ratio. The turbulent flow model with counter flow heat exchanger is considered for analysis purpose. The effect of D/d ratio on heat transfer rate and pumping power is found out for different boundary conditions. The D/d ratio is varied from 10 to 30 with an interval of 5. Nusselt number, friction factor, pumping power required and LMTD variation of inner fluid with respect to Reynolds number is found out for different D/d ratio. The optimize Reynolds number for maximum heat transfer and minimum power loss is found out by graph intersection methods. From the results complicated behavior of fluid flow is captured for both the fluids flowing inside the tube. With increases in D/d ratio (inverse of curvature ratio) the Nusselt number will decreases and the outer wall boundary condition does not have any significant effect on the inner Nusselt number. The Darcy friction factor decreases with increase in Reynolds number. The Pumping power increases with increase in Reynolds number for all the condition of D/d ratio and for all the boundary conditions. Log mean temperature difference (LMTD) increases at a steady rate with increase in Reynolds number. The optimization point between Nu and f with respect to Re; shifts toward the lower Reynolds number with increase in D/d ratio.

Key words: D/d ratio, Nusselt number, friction factor, LMTD, pumping power

TABLE OF CONTENTS

LIST OF FIGRURES

LIST OF TABLES

ABBREVIATIONS

Ac= flow area, m^2

As =surface area, m^2

Cp =specific heat, J/kg-K

d_1=diameter of inner tube, mm

d_2=diameter of middle tube or thickness tube, mm

d_3=diameter of outer tube, mm

D_h = hydraulic diameter, mm

D = coil diameter, mm

D_e =Dean Number

f =friction factor

G =mass velocity, m/s

h =heat transfer coefficient, W/m^2k

H =pitch of coil, mm

k =thermal conductivity, W/m-K

L =length of pipe, m

m =mass flow rate, kg/s

n= number of turns

Nu_x =Local Nusselt Number

Nu=Average Nusselt number

P= Pressure, N/m2

Δp= Pressure drop

Pr= Prandtl Number

q= heat flux, W/m2

Re =Reynolds Number

Re_{cr}=Critical Reynolds number

St= Stanton Number

T_{hi}=temperature of hot fluid at inlet, K

T_{ho}=temperature of hot fluid at outlet, K

T_{ci}= temperature of cold fluid at inlet, K

T_{co}= temperature of cold fluid at outlet, K

T_w= wall temperature, K

T_f= fluid mean temperature, K

u_x, u_y and u_z=velocity in x ,y, z directions

x, y, z coordinates

X, Y, Z body force in x, y, z directions

V_s = wetted volume, m^3

Greek symbol

β=surface area density, m^2/m^3

ρ =density, Kg/m^3

μ=dynamic viscosity, Kg/ms

Φ=Rayleigh dissipation factor

CHAPTER-1

INTRODUCTION

1.1. Introduction

Heat exchanger is a device which is used to transfer heat between two fluids which may be in direct contact or may flow separately in two tubes or channels. We find numerous applications of heat exchangers in day today life. For example condensers and evaporators used in refrigerators and air conditioners. In thermal power plant heat exchangers are used in boilers, condensers, air coolers and chilling towers etc. Similarly the heat exchangers used in automobile industries are in the form of radiators and oil coolers in engines. Heat exchangers are also used in large scale in chemical and process industries for transferring the heat between two fluids which are at a single or two states.

1.2. Type of heat exchangers:

- According to Heat transfer process
  1. Direct Contact Type
  2. Transfer Type Heat Exchanger
  3. Regenerators type Heat Exchanger
- According to Constructional Features
  1. Tubular Heat Exchanger
  2. Shell and Tube type Heat Exchanger
  3. Finned tube Heat Exchanger
  4. Compact Heat Exchanger

- ❖ According to flow arrangement

  1. Parallel Flow

  2. Counter Flow

  3. Cross Flow

- ❖ According to Heat transfer process

  1. Direct contact type Heat exchangers are the heat exchanger in which two immiscible fluids are directly mixed with each other to transfer heat between two fluids. The efficiency of this type Heat exchanger is more compared to other type heat exchangers. Cooling tower, jet condenser, de-super heaters, open feed water heater are the example of this type of heat exchanger.
  2. Transfer type or Recuperater type heat exchanger two fluid flows simultaneously through two tubes separated by walls.
  3. Regenerator type heat exchanger the hot and cold fluid flow alternatively on same surface. During the hot fluid transfer the wall of exchanger get heated and when the cold fluid flows through it, this heat get transferred from the wall of the heat exchanger to the cold fluid so that the temperature of cold fluid increases. The common example of this type heat exchangers are pre-heaters for steam power plant, blast furnace etc.

- ❖ According to Constructional Features

  1. Tubular heat exchangers are placed concentric to each other and two fluids flows in two tubes separated by wall. These are generally used in most of the engineering application.
  2. Shell and tube type heat exchanger consists of shell and large number of parallel tubes. The heat transfer takes places when one fluid flows through the tube and other flows outside the tube inside the shell of the exchanger this type of heat exchanger have large surface area to volume. Baffles plates are provided to enhance the turbulence hence the heat transfer rate.
  3. For improving the heat transfer rate fins are provided on the outer surface of the heat exchangers. These are generally used in gas to liquid type heat exchanger and fins are

generally provided in gas side. These are used in gas turbines, automobiles, aeroplane, heat pumps etc.

4. A compact heat exchanger can be defined as heat exchanger which has area density (β) greater than700m^2/m^3 for gas or greater than 300m^2/m^3 when operating in liquid or two-phase streams. For example automobile radiators which has an area density in order of 1100 m^2/m^3.Compact heat exchanger are generally cross flow type where two fluid flow perpendicular to each other.

❖ According to flow arrangement

1. Parallel flow type heat exchanger two fluids flow parallel to each other that is they flow in same direction. These are also called concurrent heat exchanger.
2. Counter flow heat exchanger two fluids flow in opposite direction.
3. Cross flow type heat exchanger two fluids flow perpendicular to each other. This is further divided in to mixed flow type and unmixed flow type heat exchanger

1.3. Heat transfer enhancement

Working towards the goal of saving energies and to make compact the design for mechanical and chemical devices and plants, the enhancement of heat transfer is one of the key factors in design of heat exchangers.

Heat transfer enhancement techniques are generally divided in to two types.

1. Active techniques

2. Passive techniques

In Active techniques with use of external power or some external source the heat transfer is enhanced.

For example

1. Mechanical aids

2. Surface vibrations

3. Fluid vibration

4. Electrostatic fields (DC or AC)

5. Jet impingement

Passive technique does not require any external power for enhancement of heat transfer rate. By the modifying the geometry of exchangers, by changing the surface finish or by modifying the flow by inserts or additional devices the heat transfer rate of heat exchangers can be improved.

1. Treated surfaces

2. Rough surfaces

3. Extended surfaces

4. Displaced enhancement devices.

5. Swirl flow devices

6. Coiled tubes

7. Additives for gases

8. Additives for liquids.

1.4. Helical coil heat exchanger

Recent developments in design of heat exchangers to full fill the demand of industries has led to the evolution of helical coil heat exchanger as helical coil has many advantages over a straight tube.

Advantages:

1. Heat transfer rate in helical coil are higher as compared to a straight tube heat exchanger.
2. Compact structure. It required small amount of floor area compared to other heat exchangers.
3. Larger heat transfer surface area.

1.5. Applications

1. Heat exchangers with helical coils are widely used in industries. The most common industries where heat exchangers are used a lot are power generation plants, nuclear plants, process plants, refrigeration, heat recovery systems, food processing industries, etc.
2. Helical coil heat exchanger is used for residual heat removal system in islanded or barge mounted nuclear reactor system, where nuclear energy is used for desalination of sea water.
3. In cryogenic applications including LNG plant.

1.6. Objective of work

Main aim of our project is to maximize the heat transfer rate with minimum power loss. We know that with increase in Reynolds number Nusselt number increases hence the heat transfer coefficient. But with increase in Reynolds number pumping power also increases but increase in power requirement is more compared to increases in heat transfer coefficient. So there exist a particular Reynolds number or (Dean Number) for which both the curve intersects, which is the optimum point for that particular (D/d) condition.

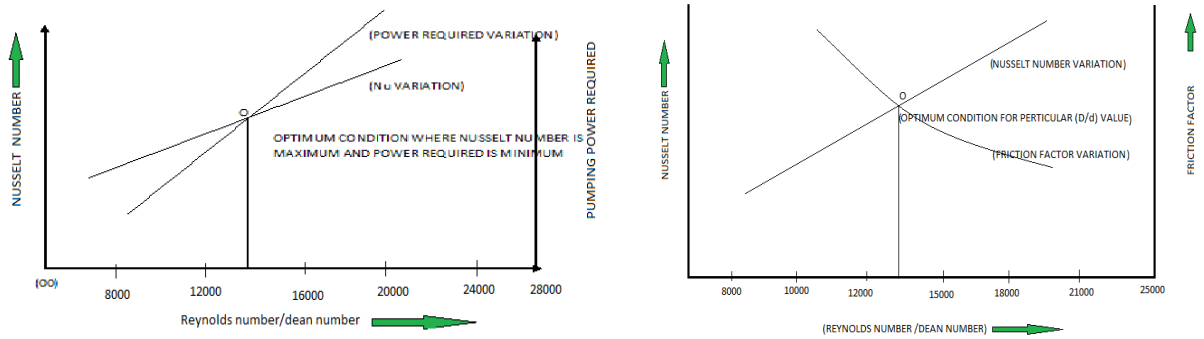

Fig. 1.1(a) optimum condition showing variation between Nu and Pumping power with respect to Re/De; (b) graph between Nu and f with respect to Re/De

Similarly this optimum condition can also be plotted between the variation of Nusselt number and friction factor with respect to Reynolds number or Dean Number.

In my project it is plotted between (Nu) & (friction factor) with respect to (Re)

Also in my project I have shown the variation of Nusselt Number, friction factor, pumping power and Log mean temperature difference with respect to Reynolds number for different D/d ratio and predict the behavior of heat transfer for varying coil diameter. The effect of different boundary condition on thermal properties of inner fluid has also studied.

Organization of the thesis

This thesis comprises of seven chapters.

In chapter -1 I have given the brief introduction of Heat exchanger, different types of heat exchangers, their applications compact heat exchanger, helical coil heat exchangers and objective of my work.

In chapter-2 I have given the Literature review on helical coil heat exchanger and the research work that has done so far in this topic.

In chapter -3 I have formulate the problem with necessary governing equation and boundary condition. I have made some basic assumption for simplicity of my problem in this chapter.

In chapter -4 I have done the CFD modeling of my problem.

In chapter -5 I explained the results and draw the conclusion for different boundary condition with help of suitable graph and figures.

In chapter-6 I draw the conclusion and mention the future scope of the project.

In chapter -7 I gave the References, abbreviations and acronyms.

CHAPTER 2

LITERATURE REVIEW

2.1. Introduction

In recent past year, the improvements in computing power have increased the interest of engineers and researchers to simulate their problems with computational and numerical methods. A lot of computational tools and methods have been developed in the last decades to analyse fluid dynamics, combustion, and different modes of heat transfer. Use of heat exchangers in wide range of applications attract the researchers and scientists to work in this field.

The helical coil-tube heat exchangers are used in industries and power sectors due to its compact structural design, larger heat transfer surface area and higher heat transfer capability. In recent past few years so much work has been done to improve the heat transfer rate of heat exchangers. Wide range of literature has been found to improve the heat transfer rate by using helical coil heat Exchanger. The secondary flow pattern of the fluid improves the heat transfer rate and the outer fluid moves with a higher velocity compared to the inner fluid due to the effect of curvature ratio. A considerable amount of experimental work has been done on flow pattern and heat transfer characteristic of Helical coil Heat Exchanger. In spite of numerical and analytical studies that have been done in helical coil tube, there are not many investigation have been done on behaviour of curvature ratio on heat transfer characteristic for different boundary conditions.

2.2. Experimental and numerical work:

Study of the heat transfer characteristics of a compact spiral coil heat exchanger under wet-surface conditions was done by Naphon and Wongwises et al. in year (2005). They had done the numerical and experimental studies to find out the heat transfer rate and predict the performance of a spiral coil heat exchangers. Cooling and dehumidifying conditions were used for analysis. They found that the rate of mass flow and temperature of air at the inlet affects the

temperature of air and water at the outlet. The outlet temperature of air and water decrease with increase in mass flow rate of water. With increase in air and water mass flow rates the enthalpy and humidity effectiveness decrease.

Kumar et al. (2006) had investigated hydrodynamic and heat transfer characteristic of tube in tube helical heat exchanger at pilot plant scale. They had done the experiment in a counter flow heat exchanger. Overall heat transfer coefficients were evaluated. Nusselt number and friction factor coefficient for inner and outer tube was found and compared with numerical value got from CFD package (FLUENT). They observed that the overall heat transfer coefficient increase with inner coil tube Dean Number for constant flow rate in annulus region.

Jayakumar et al. (2008) had done numerical and experimental work on helical coil heat exchanger considering fluid to fluid heat transfer. They had taken different boundary conditions for example constant heat flux, constant wall temperature and constant heat transfer coefficient. In their observation they found that constant value of thermal and transport properties of heat transfer medium results inaccurate heat transfer coefficient. Also the practical applications, the heat transfer in fluid to fluid heat exchangers in arbitrary boundary conditions such as constant wall temperature or constant heat flux conditions are not applicable. Based on the numerical and experimental analysis within certain error limits correlation was developed to calculate the inner heat transfer coefficient of helical coil.

Kharat et al. (2009) had done the experiments to study the heat transfer rate on a concentric helical coil heat exchanger and develop the correlation for heat transfer coefficient. Heat transfer coefficient has improved for the tube containing flue gas of the heat exchanger by using CFD simulation and the experimental study. The effect of different operating variables was studied. The variables they had considered are gap between the concentric coils, diameter of tube and coil diameter.

The heat transfer coefficients are affected by the coil gap and the tube diameter. They found that the heat transfer coefficient decreases with the increase in coil gap. With increase in tube diameter the heat transfer coefficient increases.

Jayakumar et al.(2010) had done the numerical and experimental analysis to find out the variation of local Nusselt number along the length and circumference of a helical tube. They had changed the pitch circle diameter, tube pitch and pipe diameter and their influence on heat

transfer rate was found out. They have done the prediction of Nusselt number. The of Nusselt number variation with respect to angular location of the point was also predicted in this literature.

In their conclusion they found that the heat transfer coefficient and hence the Nusselt number is not uniform along the periphery of the helical pipe. They had derived an expression to calculate the Nusselt number at various points along the periphery of the tube in the fully developed region. The effect of pipe diameter was studied and it is found that when the pipe diameter is low, the secondary flow is weak and the mixing of the fluid is less. When the diameter of the coil increases the heat transfer at the outer surface is highest. The PCD influence the centrifugal force of fluid flowing inside the tube, which in turn affects the secondary flow. When the PCD is increased, the curvature effect on flow pattern decreases and the centrifugal force plays a lesser role in flow characteristics.

Study on the flow and heat transfer characteristics in a spiral-coil tube had done by Naphon (2011). He did both the numerical and experimental study on a horizontal spiral-coil tube to predict the flow characteristic. The standard k– ε two-equation turbulence model was used to simulate the turbulent flow and heat transfer characteristics of the fluid. The heat transfer rate or heat transfer coefficient had affected by the centrifugal force. However, the pressure drop also increases. He found that the Nusselt number and pressure drop obtained from the spiral-coil tube are almost one and half times higher than that of the straight tube due to the centrifugal force.

Pawar and Sunnapwar et al. (2014) has done the Experimental analysis on isothermal steady state and non-isothermal unsteady state conditions in helical coils. They had considered both the Newtonian as well as non-Newtonian fluids for working fluid. For Newtonian fluid they considered water and glycerol–water mixture (10 and 20%glycerol). For non Newtonian fluid they considered 0.5–1% (w/w) dilute aqueous polymer solutions of Sodium Carboxy Methyl Cellulose and Sodium Alginate. The correlation was found out between the Nusselt number and nondimensional number, '*M*', Prandtl number and coil curvature ratio. They found the heat transfer rate under isothermal steady state and non-isothermal unsteady state conditions in laminar and turbulent flow conditions.

Lu et al. (2014) had done the experimental and numerical study on the shell-side thermal-hydraulic performances of multilayer spiral wound heat exchangers under different thermal boundary wall conditions.

2.3. Numerical work:

Rennie et al. (2006) had done the numerical analysis on a double-pipe helical heat exchanger. The proposed heat exchanger was investigated numerically for laminar flow condition. The heat transfer characteristics under different flow rates of fluid and tube sizes were also studied. Both parallel and counter flow heat exchanger were considered. The correlation between annulus Nusselt number with a modified Dean number was found.

Yan Li et al. (2010) had done investigations on high pressure shell-and-tube heat exchangers for syngas cooling in an IGCC. The optimization was done by using numerical techniques. In their work they had investigated the flow field and the heat transfer characteristics of a shell-and-tube heat exchanger for the cooling of syngas.

They had studied the pressure drop and the temperature variation across the heat exchanger. They had also showed that; how the syngas components affect heat transfer coefficient. From their results they found that high the operation pressure more will be the heat transfer rate. The pressure drop and the heat transfer rate of the fluid were affected by syngas. The arrangement of the baffle plates inside the exchanger also affects the flow characteristic of fluid. They found that by making the height of the baffles short, using lesser number of the baffle plates and increasing the spacing between them, can decrease the resistance.

Lee et al. (2010) had numerical studied the heat transfer performance of multi-coil condensers. Air flow characteristics are also studied for different coil configurations. In their study they had investigated the effects of different included angles between the coils of the condenser. They found that the surface area is not only the key factor to improve the heat transfer rate and performance of multi coil exchanger. From the results they found that the air flow rate can be improved by the variation of the included angle. The heat transfer rate is increased by 5.29% due to improved flow rate of air. The reduction in the stagnant flow regions of the heat

exchanger coils, and even distribution of flow throughout the coils is the main reason of improvement of heat transfer rate.

Huminic et al.(2011) had numerically investigated the heat transfer characteristics in double tube helical coil heat exchangers. Nanofluids were used as working fluid in the exchanger. They consider laminar flow condition. CuO and TiO_2 are used as nano particles in the working fluid. The concentration of nano particles affects the heat transfer rates. The Dean number which is a function of curvature ratio also affects the heat transfer coefficients in helical heat exchanger. They came to know that by the use of nano particles as working fluid the heat transfer rate can be improved from that of pure water. The convective heat transfer coefficients can be increased with increasing of the rate of mass flow. With increase in the Dean number heat transfer rate can also be increased.

Ferng et al. (2012) had done the numerical work in a helically coiled heat exchanger. Numerical investigation was focused to predict the effects of Dean number and pitch size of the tube on the thermal and hydraulic characteristics of a helical tube heat exchanger. They had considered three Dean numbers and four sizes of pitch for their study. The turbulent wake around the rear of a coiled tube, the secondary flow within the tube, and the developing flow and heat transfer behaviours from the entrance region, etc was studied by them.

Jahanmir et al. (2012) had done numerical work on shell and tube heat exchanger with single twisted tube bundle in five different twist angles, and compared the results with conventional shell and tube heat exchanger with single segmental baffles. They had studied the effect of shell-side nozzles configurations on heat exchanger performance. While analysing the results they found that, for the same shell-side flow rate, the heat transfer coefficient of heat exchanger with twisted tube bundle is lower than that of the heat exchanger with segmental baffles. Shell-side pressure drop of the heat exchanger with twisted tube bundle is even much lower than that of the heat exchanger with segmental baffles.

In their study these are some of the findings, Pressure drop decreases rapidly for heat exchanger with twisted tube bundle than that of single-segmental heat exchanger. From 25^o to 65° twist angle, the overall heat transfer coefficient and pressure drop change was negligible.

The maximum heat transfer rate for a specified pressure drop was found at the angles of 55° and 65°.

Jamshidi et al. (2012) had done numerical work to optimize design parameter of Nano fluids inside helical coils. In their study they used water/Al_2O_3 nanofluid in helical tubes. The fluid flow was assumed to be laminar. The outer wall of exchanger was maintained at constant wall temperature.Thermo physical properties of nano fluids are depend on particles volume fraction and temperature. Numerical simulations are used to investigate the effect of fluid flow and geometrical parameters. Taguchi method is also used to optimise the geometrical parameter of heat exchanger. From their results they found that the thermal–hydraulic performance of helical tubes was improved by the nano fluids. But the nano fluids don't change the optimized shape factors.

In this study thermal–hydraulic performance of helical coil by using water and water/ Al_2O_3 Nanofluid are investigated numerically and optimize by using Taguchi method. The thermal conductivity and the viscosity of Nanofluid are affected by adding Nanofluid. From the results it is conformed that adding nanoparticles improve the thermal–hydraulic performance.
The important design parameters for a helical coil tube with specified tube diameter and longitude length are coil diameter and coil pitch.

Yang San et al. (2012) had numerically investigated the heat transfer characteristics of a helical heat exchanger. The performance of a helical heat exchanger was investigated on the basis of heat transfer rate. The cross section of the tube was made rectangular section with two cover plates. They found that the friction factor was increased with the increase in spacing of the channel. The friction factor decrease with increase in the Reynolds number. They found Nu was increase with increase in Re and channel spacing.

A numerical investigation on the effect of natural convection induced on the outer side heat transfer rate of coiled tube heat exchangers was done by Zachar in year (2012). He found that the inner fluid flow rate of helical tube heat exchanger affect the outside heat transfer coefficient. Average Nusselt number along the helical tube depends up on the heat flow direction.

Aly et al. (2014) had done the numerical study to find the heat transfer and pressure drop of nano fluid in coiled tube-in-tube heat exchangers for turbulent flow condition. The numerical study was carried out by computational fluid dynamics (CFD) analysis to find the heat transfer rate and pressure drop characteristics of water-based Al_2O_3 nano-fluid flowing inside coiled tube-in-tube heat exchangers. The overall performance the heat exchangers was assessed based on the thermo-hydrodynamic performance index. Nanofluid flows inside inner tube side. When he compared the result for the same Re or Dn, the heat transfer coefficient or the rate of heat transfer was increased by increasing the coil diameter and nanoparticles volume concentration. Also, he found that the friction factor increases with the increase in curvature ratio and the pressure drop penalty is negligible with increasing the nano-particles volume concentration up to 2%. For the nano fluid the correlations for predicting average heat transfer and friction factor in turbulent flow regime such as Gnielinski correlation and Mishra and Gupta correlation, respectively, for helical tubes are also valid. In results they found that nanofluids behave like a homogeneous fluid.

2.3. Experimental works:

Jayakumar and Grover et al. (1997) had investigated the performance of residual heat removal system for two phase natural circulation. They had done their experiments on helical coil heat exchanger. They had studied the effect of different process parameter on heat transfer characteristics.

Enhancement of heat transfer rate by inserting the helical tapes had been studied by Eiamsa-ard et al. (2005) for straight tube. They experimentally found that helical tape inserted in the inner tube of the heat exchanger enhance the heat transfer rate by inducing the swirl motion. This induced swirl motion will increase the turbulence and hence the Nusselt number.

Effect of helical screw tape with or without core rod inserts on heat transfer performance had been studied experimentally by Eiamsa-ard et al. (2006). They also studied the effect of screw tape with or without core rod on friction factor.

Ghorbani et al. (2010) had done the experimental study to predict the behavior on the mixed convection heat transfer in a coil-in-shell heat exchanger. They chose the operating

parameters for the analysis are Reynolds, Rayleigh numbers and also the tube-to-coil diameter ratios. They had done the steady-state analyses and they had done the experiments for both laminar and turbulent flow. It was found that the mass flow rate of tube-side to shell-side ratio was effective on the axial temperature profiles of heat exchanger. From the results they had concluded that both the ε−NTU relation of the mixed convection heat exchangers and that of a pure counter-flow heat exchanger are same. From the result they had concluded that for mass flow rate ratio (R_m) which is the ratio between tube side to shell side greater than unity, the temperature profiles were in quadratic form. The temperature profiles were linear for R_m close to unity. Logarithmic form of temperature profiles was observed when the mass flow rate ratio was less than unity. The logarithmic mean temperature difference (LMTD) ratio was decreased with increase in mass flow rate.

Yang et al. (2011) had done experimental work to predict the characteristics of convective heat transfer in heat exchanger. They consider a heat exchanger with membrane helical coils and membrane serpentine tubes. The efficiency of the power generating system was affected by heat transfer performance of syngas cooler. They had done the experimental investigation on heat transfer in convection cooling section of pressurized coal gasifier with the membrane helical coils and membrane serpentine tubes under high pressure. They found that the working pressure, gas composition and flow symmetry influence the convection heat transfer coefficient of high pressure gas. By analyzing the results they found that the under the same conditions heat transfer coefficient of heat exchanger with membrane helical coils is greater than that of the heat exchanger with membrane serpentine-tube. They found that the heat transfer coefficient increment was due to the increase of gas pressure and velocity.

Srbislav et al. (2012) had done the experimental work predict the performances of heat exchangers with helical tube coils. In their work they had presented the results of thermal performance measurements on 3 heat exchangers with concentric helical coils. It was found that the shell-side heat transfer coefficient was affected by the geometric parameters. Winding angle, radial pitch and axial pitch are the geometric parameters which affect the heat transfer coefficient. From the results it was concluded that the shell-side heat transfer coefficient is based on shell side hydraulic diameter.

Final form of shell-side heat transfer correlation proposed by Srbislav et al. (in which Nusselt and Reynolds numbers are based on hydraulic diameter) is given by,

$$Nu = 0{:}50 Re^{0:55} Pr^{1/3} \left(\eta / \eta_w \right)^{.14}$$

Jamshidi et al. (2013) had done experimental work enhance the heat transfer in shell and helical tube heat exchanger. In the helical tube section of the heat exchanger hot water flows. The cold water flows in the shell side of the heat exchanger. The heat transfer coefficients are determined using Wilson plots. Taguchi method is used to find the optimum condition for the desired parameters in the range of $0.0813 < Dc < 0.116$, $13 < Pc < 18$, tube and shell flow rates from 1 to 4 litter per minute. From their results it is found that the higher coil diameter, coil pitch and mass flow rate in shell and tube can enhance the heat transfer rate for this type of heat exchanger. Contribution ratio obtained by using Taguchi method and it shows that shell side flow rate, coil diameter of helical coil, tube side flow rate and coil pitch are the most important design parameters in coiled heat exchangers.

From the experimental work it was found that, as the coil pitch affect the Nusselt number and the fluid rate of flow affects this variation. The highest tube side Nusselt number is obtained by the lowest coil pitch and highest tube side flow rate due to higher torsion in lower pitches. By decreasing the coil pitch, the curvature of tube increases and stronger secondary flow is produced in tube side. The secondary flow is the principal reason for enhancement of heat transfer rate in helical tubes. The tube side Nusselt number and overall heat transfer coefficient increases by increasing the coil diameter of the tube.

From the literature we find that so much work had been done to find heat transfer characteristic of helical coil heat exchanger with constant wall temperature and constant heat flux conditions. Also by changing the working fluid heat transfer relation were found. But effect of outer boundary wall condition on inner fluid has not been yet predicted properly. The effects of D/d ratio on thermal properties are not studied properly. The optimize condition based on Nusselt number and friction factor for different D/d conditions are not found out yet.

CHAPTER:-3

PROBLEM FORMULATION

3.1 Introduction

In the literature survey we found that so much work had been done to enhance the heat transfer rate in heat exchanger. But there is no work has been done to optimize the heat transfer rate with respect to power consumption. In my work I optimize the given helical coil heat exchanger keeping in mind that it should produce maximum heat transfer rate with minimum power consummation. Because some times in the process of improving the heat transfer coefficient we consume more power without knowing the economical cost.

3.2 problem specification

In my study I consider the double tube helical coil heat exchanger or tube in tube helical coil heat exchanger with two (2) numbers of turns. For simplification in numerical analysis I consider only two turns but in practical problems it may be large number of turns depending on the requirements. The coil diameter (D) was varying from 80mm to 240mm in an interval of 40mm that is120mm, 160mm, 200mm respectively. As the coil diameter increases the length of the exchanger (L) also increases. The inner tube diameter (d_1) was 8mm. the thickness (t) of the tube was taken 0.5mm. The outer tube diameter (d_2) was taken 17mm. In my study I fixed the tube diameter (both inner and outer diameter) of the heat exchanger and vary the coil diameter of the tube to see the effect of curvature ratio (d/D) on heat transfer characteristics of a helical coil heat exchanger. The pitch of the coil was taken 30mm that is the total height of the tube was 60mm. The heat exchanger was made of COPPER. The fluid property was assumed to be constant for analysis.

After creating the geometry and doing the meshing in ANSYS 13 the problem was analyzed in ANSYS 13 (FLUENT) for different boundary conditions as specified later. For analysis of the problem turbulent fluid flow condition was considered.

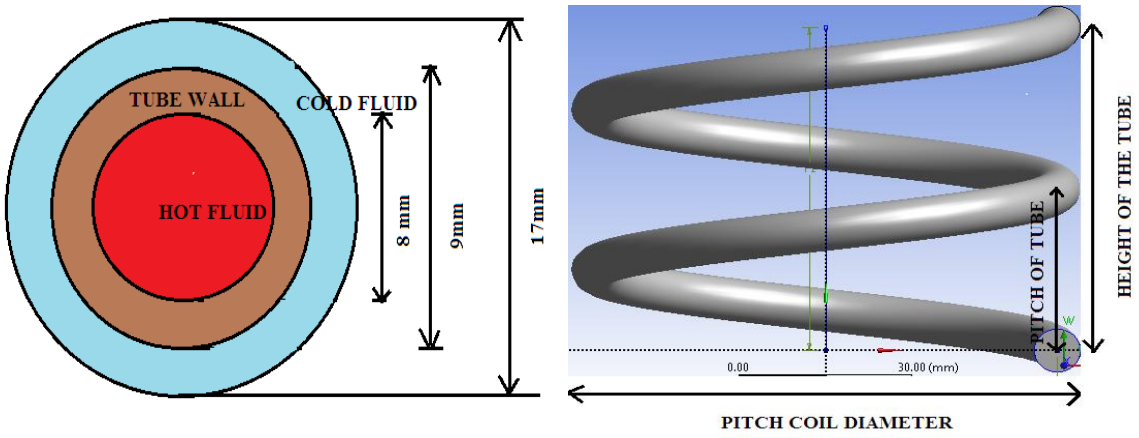

Fig.3.1 Front view of helical coil heat exchanger showing different fluid flowing and geometrical parameters with dimensions

In recent past few years study of heat exchanger with parallel flow and counter flow has been done to predict the heat transfer behavior. In this study I considered the counter flow heat exchanger as it has better heat transfer rate compared to parallel heat exchanger. The cold fluid and the hot fluid flow in opposite directions in their respective tube. In this study for analysis, turbulent fluid flow was considered. Both the hot fluid and cold fluid flow with a velocity, for which Reynolds number is greater than critical Reynolds number as per the correlation calculated by Schmidt, (1967). The flow velocity of cold fluid is remained constant and the hot fluid flow rate varied to find the heat transfer rate, friction factor and optimize the heat exchanger to have minimum pressure loss and maximum heat transfer.

Though it is a three dimensional problem but for showing the boundary condition in a simple manner it is represented in two dimensional figure.

(a) (b)

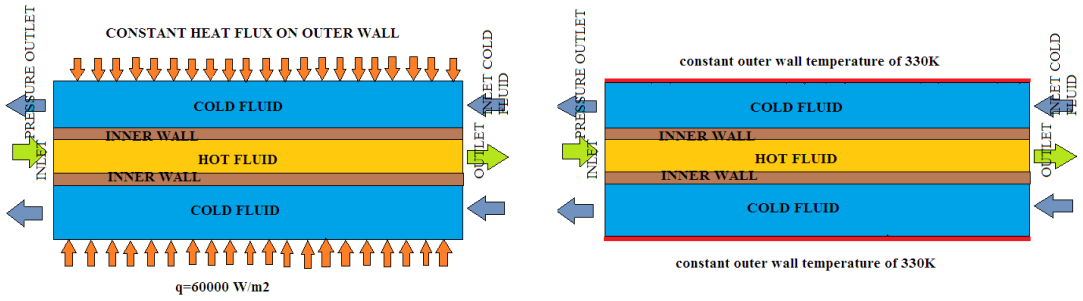

(c) (d)

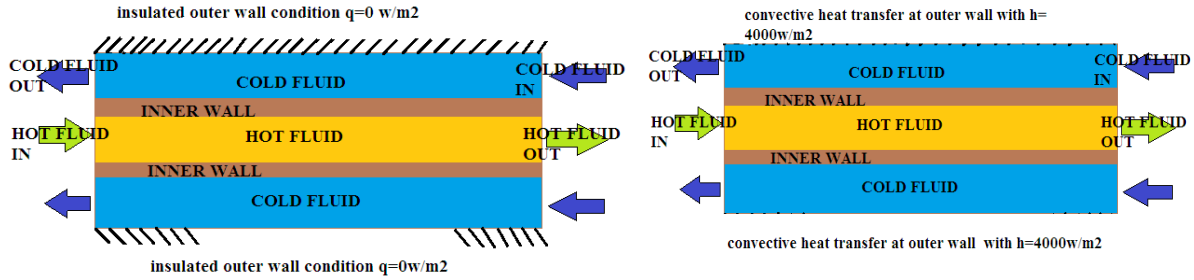

Fig. 3.2(a) constant wall heat flux condition, (b) constant wall temperature boundary condition, (c) insulated outer wall condition, (d) convective heat transfer coefficient condition at outer wall

3.3 Boundary conditions

The analysis of the model was done under following section.

For outer wall following four conditions was taken;

Case 1: The outer wall of the heat exchanger has taken constant wall temperature of 330K, as shown in Fig. 3.2(b). It can be expressed numerically by; at d_3=17mm; T=330K

Case 2: The outer wall of heat exchanger has taken constant heat flux of 60000 W/m^2, as shown in Fig. 3.2 (a). That is at d_3=17mm; q=60000W/$m^{2.}$

Case 3: Insulated outer wall was taken in the next condition, as given in the Fig. 3.2 (c). At d_3=17mm; q=0W/m^2.

Case 4: constant heat transfer coefficient of 4000W/m^2K was taken for outside atmosphere, as shown in Fig.3.2 (d). That is at d_3=17mm; h=4000W/m^2K.

For inner wall **conjugate heat transfer**, boundary condition was taken. In this condition the heat is transferred from one fluid to the other fluid via a solid (wall of the tube) so that the cold fluid get warmer and the hot fluid get colder.

For inlet of hot fluid **velocity inlet** condition was taken. Here the velocity of the fluid was varied by changing the Reynolds number (Re). For turbulent fluid flow the critical Re was found out by using the Schmidt correlation as given by equation no- 3.9. The Reynolds number of the working was fluid assumed at the inlet are 10000,12000,15000,18000,21000,24000,25000 respectively. As the Reynolds number changes the mass flow rate of the hot fluid also changes and maximum for Re=25000. The hot fluid temperature at inlet was taken 355 K. Representing this condition in mathematical form we have;

At x, y, z=0; $u_x=u_y=0$ and u_z=1.25601, 1.55072, 1.884, 2.26081, 2.6376, 3.01442, 3.14002m/sec respectively and T_{hi}=355K

Similarly for the cold fluid at the inlet **velocity inlet** condition was also taken. For the cold fluid the fluid flow rate was assumed to be constant. The Reynolds number for the outer fluid was taken 25000 for all the condition of fluid flow. The mass flow rate of the cold fluid was found to be 0.512105 kg/sec. The temperature of the fluid at the inlet is taken 290 K.

At exit, Re=25000 or $u_x=u_y=0$ and $u_{z=}$-3.14002m/sec and T_{ci}=290

For outlet of the cold and hot fluid **pressure outlet** boundary condition was taken. At the outlet the gauge pressure was taken zero atmospheric pressure.

The side wall of the heat exchanger was taken **insulated wall** condition, because there is no heat transfer takes place to and from this side of the exchanger.

At x=y=0 and d_1=8mm to d_2=9mm; q=0W/m^2

The fluid properties of the working fluid (water) was assumed to be constant throughout the analysis with respect to temperature and presented in the table 3.1.

Table 3.1 Properties of water:

DESCRIPTION	VALUE	UNITS
VISCOSITY	0.001003	kg/m-s
DENSITY	998.2	kg/m^3
SPECIFIC HEAT CAPACITY	4182	J/kg-K
THERMAL CONDUCTIVITY	0.6	W/m-K

The tube of the heat exchanger was made up of copper for maximize the heat transfer, because copper has good thermal conductivity. Also the properties of the copper were also remains constant throughout the analysis. It is represented in table 3.2.

Table 3.2 Properties of copper:

DESCRIPTION	VALUE	UNITS
DENSITY	8978	kg/m^3
SPECIFIC HEAT CAPACITY	381	J/kg-K
THERMAL CONDUCTIVITY	387.6	W/m-K

3.4 Basic assumptions

1. Outer wall thickness is neglected for simplifying the numerical calculation.
2. Flow through the helical coil Heat Exchanger is considered as Turbulent flow.
3. Steady state heat transfer conditions were assumed.
4. Incompressible fluid with constant fluid property.
5. Natural convention and Radiation was neglected.
6. Conjugate heat transfer between the two fluids was considered.
7. Counter flow heat exchanger was considered.

3.5 Governing equations:

The governing differential equation for the fluid flow is given by Continuity equation or mass conservation equation, Navier Stokes equation or momentum conservation equation and energy conservation equation.

1. **Continuity equation**:

$$\frac{\partial(\rho u)}{\partial x}+\frac{\partial(\rho v)}{\partial y}+\frac{\partial(\rho w)}{\partial z}=0 \qquad \textbf{(3.1)}$$

2. **Navier Stokes equation:**

$$\rho\left(u\frac{\partial u}{\partial x}+v\frac{\partial u}{\partial y}+w\frac{\partial u}{\partial z}\right)=\rho x-\frac{\partial p}{\partial x}+\frac{1}{3}\mu\frac{\partial}{\partial x}\left(\frac{\partial u}{\partial x}+\frac{\partial v}{\partial y}+\frac{\partial w}{\partial z}\right)+\mu\nabla^2 u$$

$$\rho\left(u\frac{\partial v}{\partial x}+v\frac{\partial v}{\partial y}+w\frac{\partial v}{\partial z}\right)=\rho Y-\frac{\partial p}{\partial y}+\frac{1}{3}\mu\frac{\partial}{\partial y}\left(\frac{\partial u}{\partial x}+\frac{\partial v}{\partial y}+\frac{\partial w}{\partial z}\right)+\mu\nabla^2 v$$

$$\rho\left(u\frac{\partial w}{\partial x}+v\frac{\partial w}{\partial y}+w\frac{\partial w}{\partial z}\right)=\rho Z-\frac{\partial p}{\partial z}+\frac{1}{3}\mu\frac{\partial}{\partial z}\left(\frac{\partial u}{\partial x}+\frac{\partial v}{\partial y}+\frac{\partial w}{\partial z}\right)+\mu\nabla^2 w \qquad \textbf{(3.2)}$$

3. **Energy equation**:

$$\rho c_p\left(u\frac{\partial T}{\partial x}+v\frac{\partial T}{\partial y}+w\frac{\partial T}{\partial z}\right)=\left(u\frac{\partial p}{\partial x}+v\frac{\partial p}{\partial y}+w\frac{\partial p}{\partial z}\right)+k\nabla^2 T+\mu\phi \qquad \textbf{(3.3)}$$

Where;

$$\phi=2\left[\left(\frac{\partial u}{\partial x}\right)^2+\left(\frac{\partial v}{\partial y}\right)^2+\left(\frac{\partial w}{\partial z}\right)^2\right]+\left[\left(\frac{\partial u}{\partial y}+\frac{\partial v}{\partial x}\right)^2+\left(\frac{\partial v}{\partial z}+\frac{\partial w}{\partial y}\right)^2+\left(\frac{\partial w}{\partial x}+\frac{\partial u}{\partial z}\right)^2\right]$$

$$-\frac{2}{3}\left[\frac{\partial u}{\partial x}+\frac{\partial v}{\partial y}+\frac{\partial w}{\partial z}\right]^2$$

The governing differential equation for solid domain is only the Energy equation which is given by;

$$\nabla^2 T = 0 \qquad \textbf{(3.4)}$$

Heat transfer coefficient is obtained by equating the conduction heat transfer to the convection heat transfer;

$$q_{cond} = q_{conv}$$

$$h = \frac{-k\dfrac{\partial T}{\partial x}}{T_w - T_f} \qquad \textbf{(3.5)}$$

Local Nusselt number is given by;

$$Nu_x = hD/k \qquad \textbf{(3.6)}$$

Or it can also be represented by following equation

$$Nu_x = \frac{-\dfrac{\partial T}{\partial x} d_h}{T_w - T_f}. \qquad \textbf{(3.7)}$$

Then the average Nusselt number can be found by following relation;

$$Nu_{avg} = \frac{1}{L}\int_0^L Nu_x dx \qquad \textbf{(3.8)}$$

Critical Reynolds number as per the Schimidt correlation (1967);

$$Re_{cr} = 2300[1+8.6(d/D)^{0.45}] \qquad \textbf{(3.9)}$$

Using this relation following graph can be obtained for different curvature (d/D) ratio;

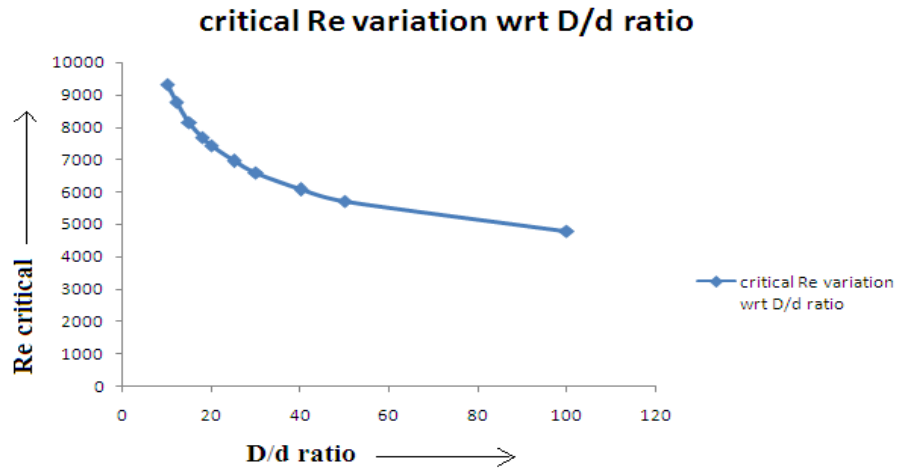

Fig. 3.3 variation of Re_{cr} with respect to D/d ratio using Schmidt correlation

Friction factor is given by;

$$f = \frac{2 \times \Delta p \times d}{\rho L v^2} \tag{3.10}$$

Length of pipe is given by following relation;

$$L = n\sqrt{H^2 + (\pi D)}^2 \tag{3.11}$$

Log Mean Temperature Difference for counter flow heat exchanger can be presented by following relation

$$LMTD = \frac{\Delta T_1 - \Delta T_2}{\ln \frac{\Delta T_1}{\Delta T_2}} \tag{3.12}$$

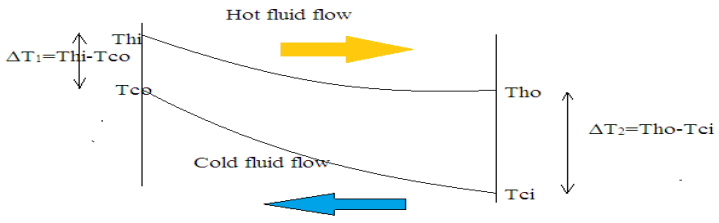

Fig. 3.4 Log mean temperature difference of hot and cold fluid

Where $\Delta T_1 = T_{hi} - T_{co}$

and $\Delta T_2 = T_{ho} - T_{ci}$

To find the outlet fluid temperature we can use the energy balance equation,

$$Q = mC_p(T_1 - T_2) = hA_s(T_w - T_f) \quad \textbf{(3.13)}$$

CHAPTER -4

CFD MODELING

4.1 Introduction

The invention of high speed computers, combined with the accurate numerical methods for solving physical problems, has revolutionized the way we study and practice fluid dynamics and heat transfer problems. This is called Computational Fluid Dynamics (CFD), and it has made it possible to analyze complex flow geometries with the same ease as that faced while solving idealized problems using conventional methods. CFD may thus be regarded as a zone of study combining fluid dynamics and numerical analysis. Historically, the earlier development of CFD in the 1960s and 1970s was driven by the need of the aerospace industries. Modern CFD, however, has applications across all disciplines – civil, mechanical, electrical, electronics, chemical, aerospace technology, ocean science, and biomedical engineering being a few of them. CFD substitutes analytical studies and experimental testing, and reduces the total time of testing and designing.

All the CFD software contain three basic elements

1. Pre processor
2. Main Solver
3. Post processor

The process of CFD modeling starts with an understanding of the actual problem and identifying the computational domain. This step is followed by generations of the mesh structure, which is the most important portion of the pre-processing activity. Both computation time and accuracy of solution depend on the mesh structure. That is finer the grid is more accurate the result is. But the grid size should not made unnecessary finer so that the computation takes extra time for computing, there should be an optimal grid size in which all the computation should be done.

The solver is the heart and mind of CFD software. It sets up the equations which are selected according to the options chosen by the analyst and grid points generated by the pre-processor, and solves them to compute the flow field.

The post-processor is the final part of CFD software. It helps the user to analyze the results and get useful data and draw the conclusion. The results may be displayed as vector plots of vector quantities like velocity, contour plots of scalar variables, for example pressure and temperature, in case of unsteady simulation. Global parameters like friction coefficient, Nusselt number and Colburn factor etc. may be computed through appropriate formulas.

4.2 CFD procedure

For numerical analysis in CFD following five stages are required

4.2.1 Geometry creation

In geometry creation we have to create the helical pipe. For this we have to open the ANSYS 13, go to CFD fluent package and open the DESIGN MODLER then change the property to three dimensional. In DM first we have to create the profile for our problem circle is he profile. So to create the circle select the XY-plane then set the unit to millimeter. Then go to sketching and draw the circle then specify the dimension for example its radius, and distance of the circle from XY-axis. Then generate the circle. Similarly generate other two circles for outer tube. For generating the path draw a line perpendicular to XY-plane. Give it dimension as mention in the problem.

For generating the helical tube we have to do the SWEEP procedure. For sweep we have to select the profile and the path, then operation should be ADD FROZEN. Then specify the number of turns, for this problem we select two numbers of turns. Then generate it to create the helical pipe. Same procedure is followed for generating the two annulus helical tubes. After generating the three tubes specify the body type that is whether it is FLUID or SOLID. The outer and innermost tubes are in FLUID condition and middle tube is in SOLID state.

To create the annular tube go for the BOOLEAN operation and subtract the inner tube from outer tube whiling preserving the tool body. In FLUENT for heat transfer we need conjugate heat transfer condition for this we have to make the three parts three bodies to one part

three bodies. For this select three bodies and right click on it then form NEW PART. Then save the project and close the DESIGN MODLER.

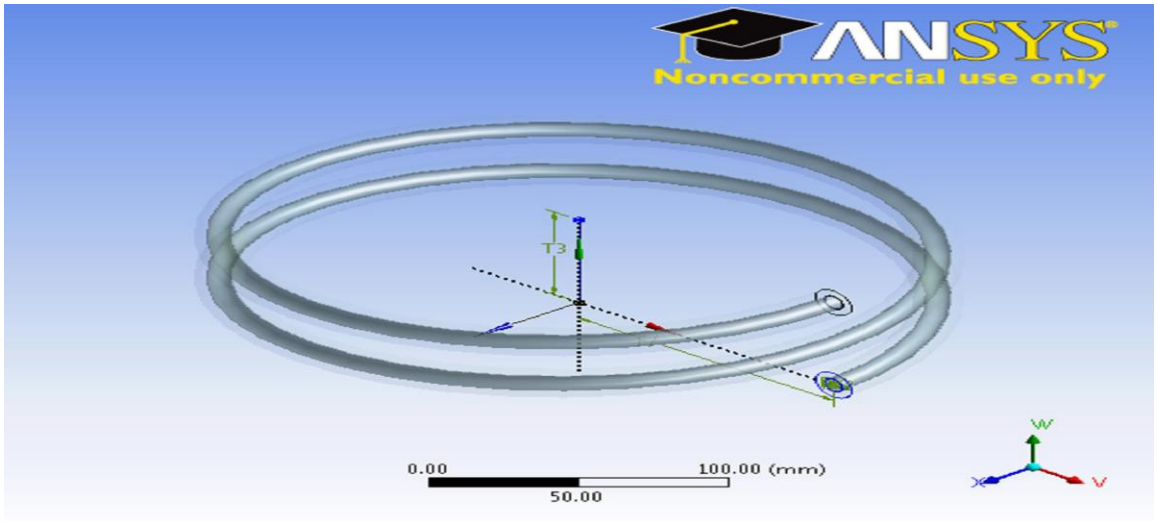

Fig. 4.1 showing the geometry of double tube helical coil heat exchanger created in ANSYS 13 work bench.

4.2.2 Grid generation

In grid generation first go to the MESH option located in FLUENT tree then press the GENERATE MESH button. It will create automatic grid. Then we have to modify the grid or make the grid finer so that accurate results will come. For generating fine mesh go for the sizing option then select the EDGE for making the division. Then specify the number of divisions.

For generating the uniform mesh we have to MAP the face, for that we have to select the MAPPED FACE option and select the face for which we have to do the operation. This will create uniform mesh throughout the face of the geometry. Similarly in MESHING METHOD we can specify the type of mesh we want to create for example QUAD, TRI, QUAD/TRI etc.

After that we have to name each face of the geometry. For that right click on the face and go to CREATE NAME SELECTION then name each face (for example inlet, outlet, wall etc). Then update the project.

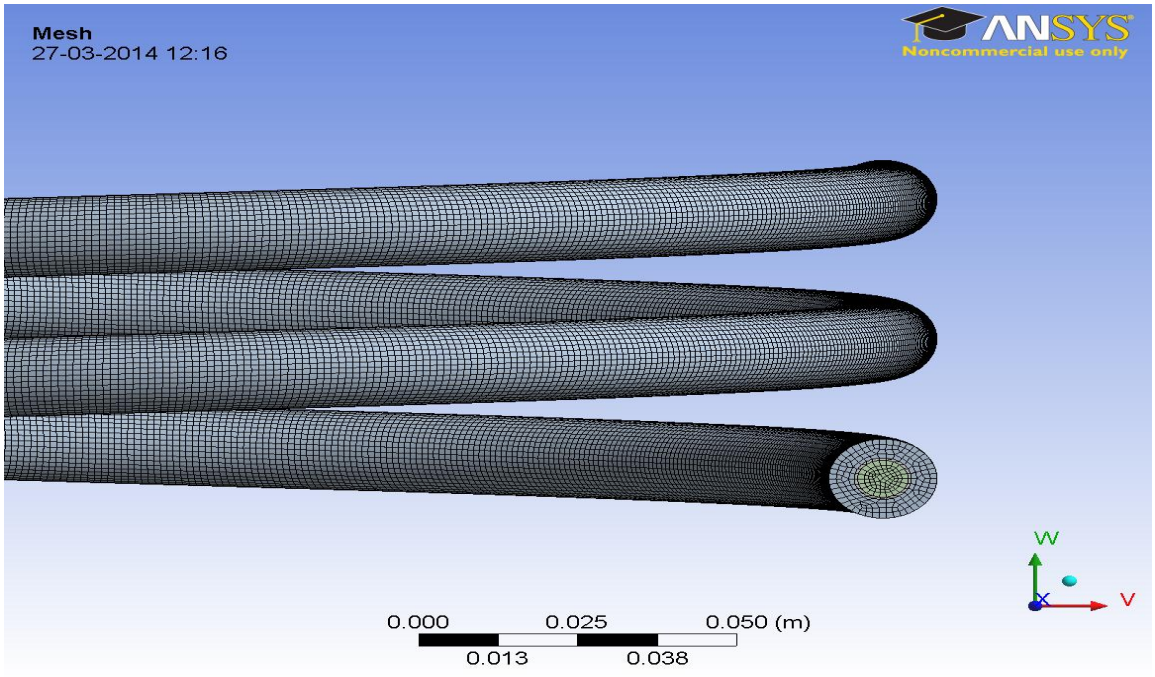

Fig 4.2 grid generation for the double tube helical coil heat exchanger

4.2.3 SETUP AND FLOW SPECIFICATION

In SETUP we generally set the operating conditions, flow specifications, boundary conditions, define the appropriate model for solving the problem.

First open the SETUP and specify it DOUBLE PRESSION for more accurate answer.

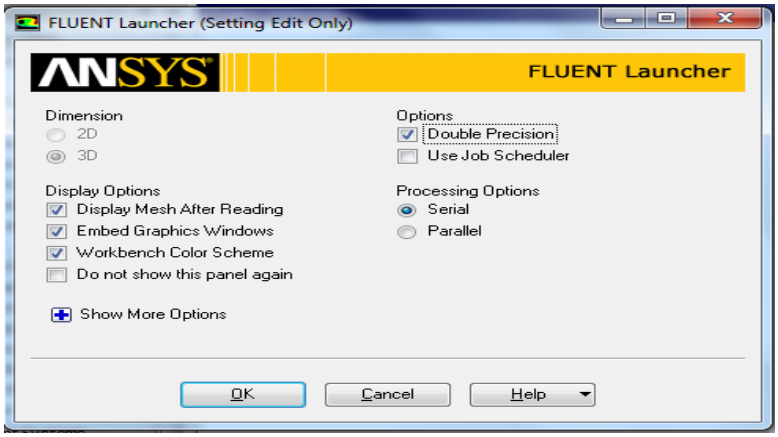

Then in the problem set up tree go for the GENERAL option and change the scale form meter to millimeter.

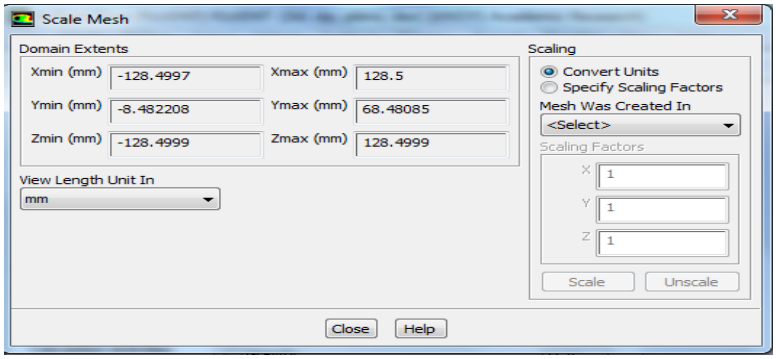

In the MODEL tree option the energy equation should be turned on for calculating the temperature profile for the heat exchanger.

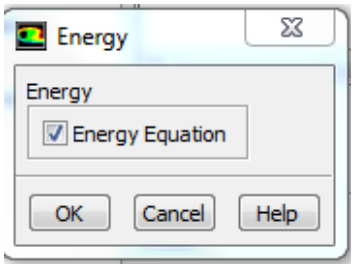

For turbulent model standard K- ε model was used. For this viscous model standard k- ε model was turned on.

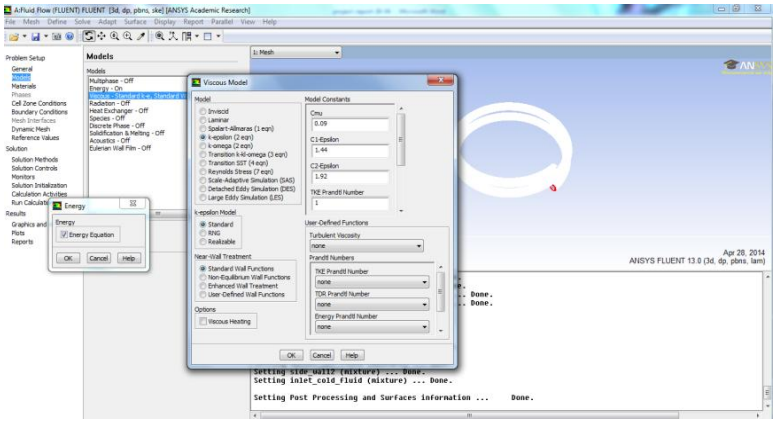

For selecting the material we have to go for problem set up tree and then go for the MATERIAL option then go for change and edit option where we can select the material from fluent database.

After selecting the suitable material (copper for solid and water for fluid), we can change their property according to our requirements.

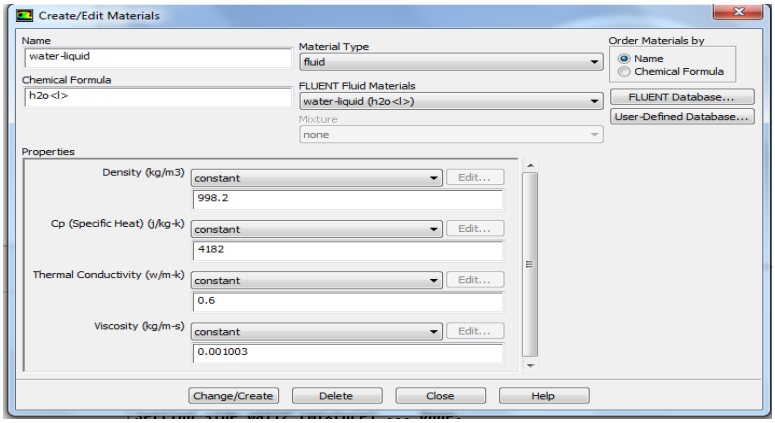

Then we have to specify the domain or the cell zone condition. For inner and outer fluid it should be water-fluid and for solid it should be copper.

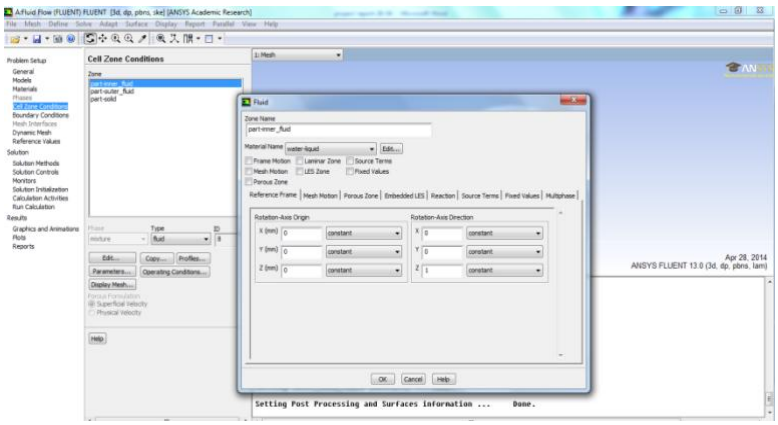

For setting the boundary condition go to BOUNDARY CONDITION option in problem set up tree then chose the different boundary condition zone with specifying the type of boundary (velocity inlet/pressure outlet/wall) etc. Then in each boundary condition go for EDIT option then specify the values according to the requirements.

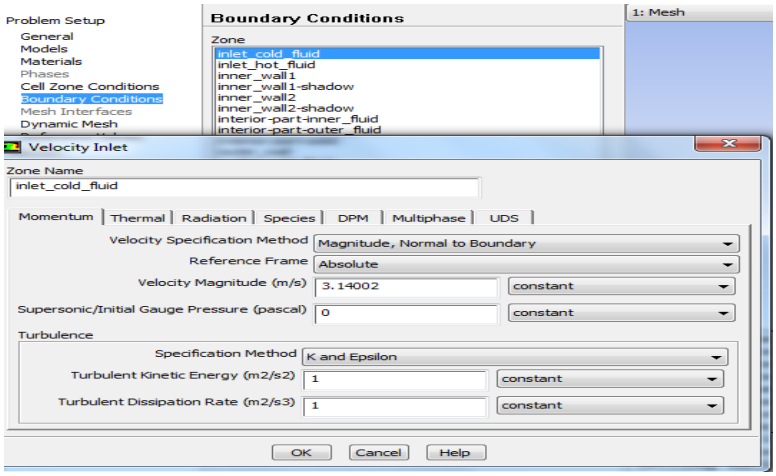

After the problem set up part is over then go for the SOLUTION tree option.

In solution tree option we have to specify the SOLUTION METHORD. For this case we considered the pressure velocity scheme as SIPMLEC with skewness correction factor as 1. In spatial discretization the GRADIENT should be LEAST SQUARE CELL BASED, pressure should be LINEAR, momentum, turbulent kinetic energy, turbulent dissipation energy should be POWER LAW and energy equation should be SECOND ORDER UPWIND scheme.

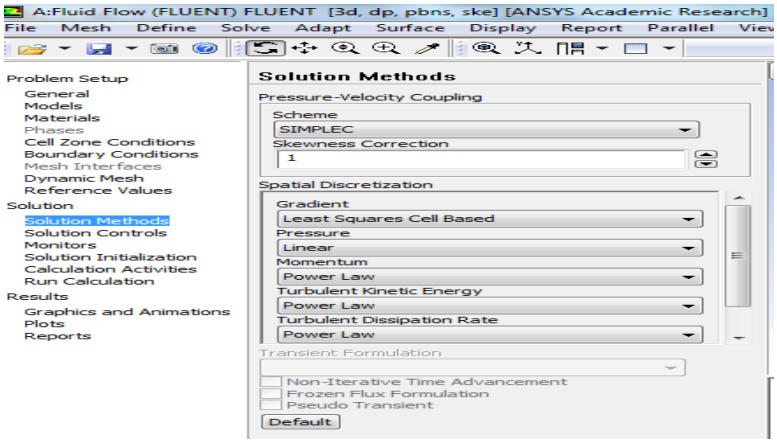

To specify the accuracy level the monitor option was selected and in monitor option RESIDUAL, PLOT option was selected. In RESIDUAL PLOT the accuracy level was set to10^{-6} for continuity, X, Y, Z momentum equation, turbulent dissipation and turbulent kinetic energy equation. For energy equation accuracy level should be 10^{-8}.

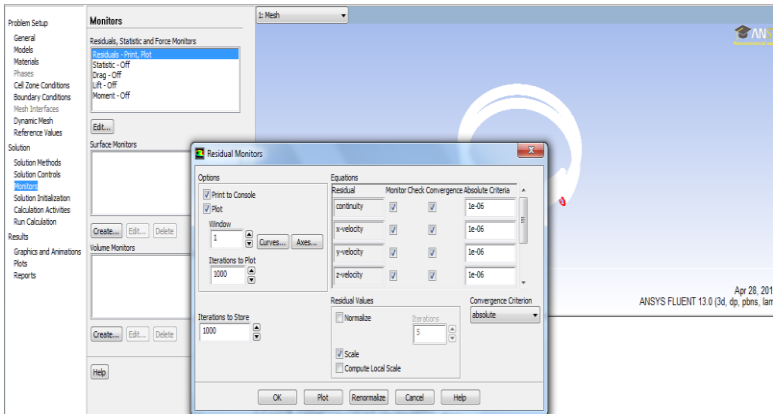

In the next step the problem should be initialized by SOLUTION INITIALIZATION option. For this problem initialization method was STANDARD INITIALIZATION and the computation starts from **inlet hot fluid** with reference frame of **relative to cell zone.**

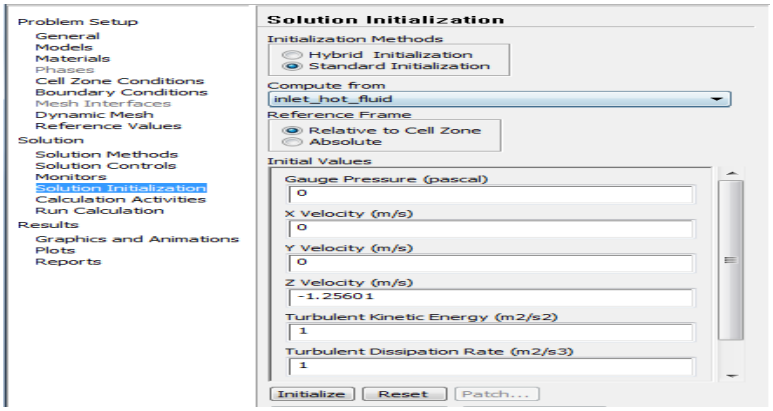

After the solution is initialized the calculation should be done by giving the number of iterations. When the solution is conversed the results can be found out from GRAPHICS AND ANIMATIONS and REPOTRS options.

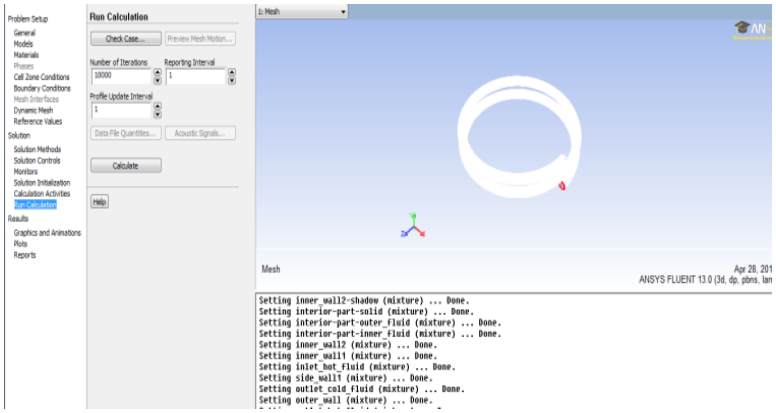

4.3. Grid independence test

Grid independence test is the one of the most important test which should be done in numerical analysis of a problem. Grid independence test was done to check the final results should be independent of the number of grids. In numerical problem the results are always dependent on the number of grids generated. So if we change the number of grid the results were changed. While changing the number grids a stage may come when the results are independent of the number of grids. These minimum number of grids after which there is no change in results were observed was known as optimum grid size and the results were independent of grids.

In this problem first the grid independence test were carried out for different D/d ratio. Starting from D/d=10; considering outer wall insulated condition and keeping the inlet velocity of hot fluid at 1.5072m/sec (Re=10000) and temperature at 355K the grid size was varied from 64770 to 138775. The properties considered for checking the grid independence are temperature of cold and hot fluid at the outlet, pressure at inlet and outlet of hot fluid.

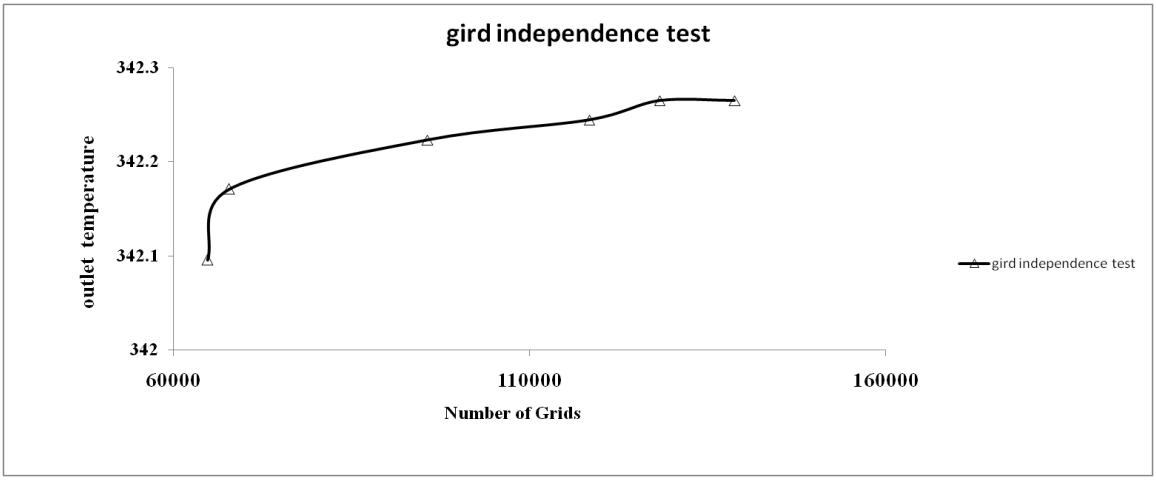

Fig. 4.3(a) grid independence test based on the outlet of hot fluid temperature

In above two graphs outlet fluid temperatures were taken in Y axis and number of grids in X axis. The grids divisions were increased and corresponding temperature of hot fluid in Fig.4.3 (a) and outlet of cold fluid temperature in Fig. 4.3 (b) were shown. After 138700 numbers of divisions the results not depend on grids hence result is grid independent.

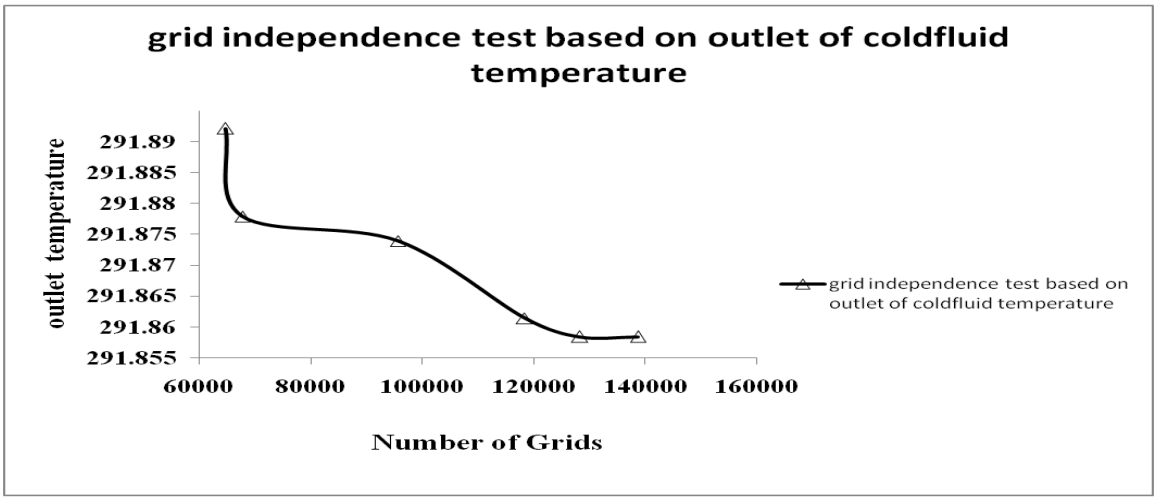

Fig. 4.3 (b) grid independence test based on outlet of cold fluid temperature

Fig.4.3(c) shows the grid independence test based on inlet pressure of hot fluid. After 137600 numbers of divisions the results not depend on grids hence result is grid independent

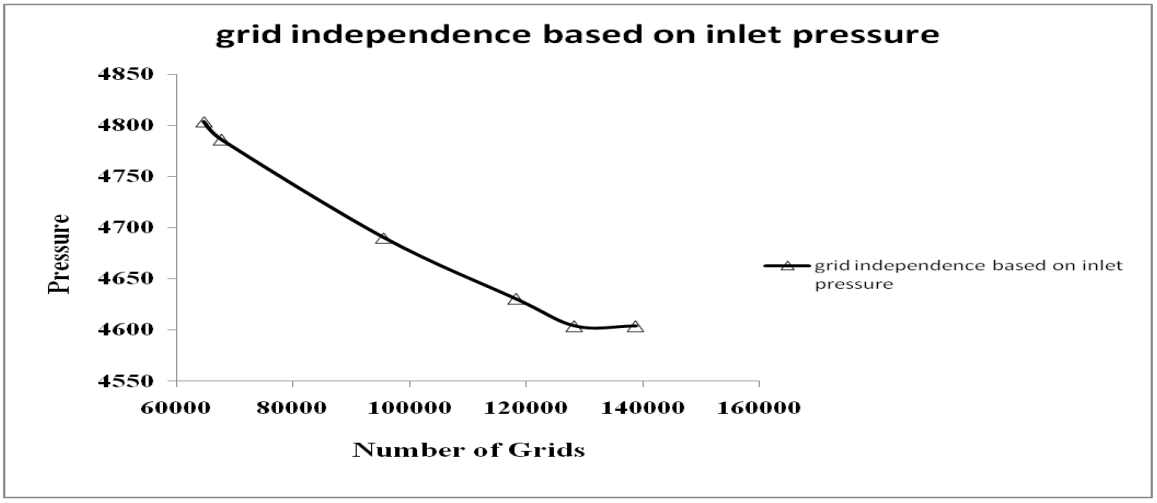

Fig. 4.3(c) grid independence test based on the pressure of hot fluid at inlet

Similarly for other D/d ratio the grid independence test has been done on the basis of outlet temperature of hot fluid and cold fluid and optimum grids were chosen for further numerical analysis.

CHAPTER-5

RESULTS AND DISCUSSION

5.1. Validation

Before starting my actual work the model proposed by me should be validated by some past work that has been already done. For this purpose I have selected the work done by Vimal Kumar et al. (2006) and Jaykumar et al. (2008).

The inner Nusselt number was calculated and compared with the Nusselt number predicted by Kumar et al. (2006) and it is found that the calculated results match with the predicted results with reasonable accuracy. Here in the fig.5.1 (a) Nusselt number is taken in Y axis and Dean number which is a function of Reynolds number and curvature ratio is considered on X axis. With increase in Dean number the Nusselt number increases. In both the cases of calculated results matches fair accurately with the results given by Kumar et al. (2006). In fig. 5.1(b) validation is done for inner Nusselt number with the work done by Jaykumar et al. (2008) for constant wall temperature conditions. It fairly agrees with the predicted results.

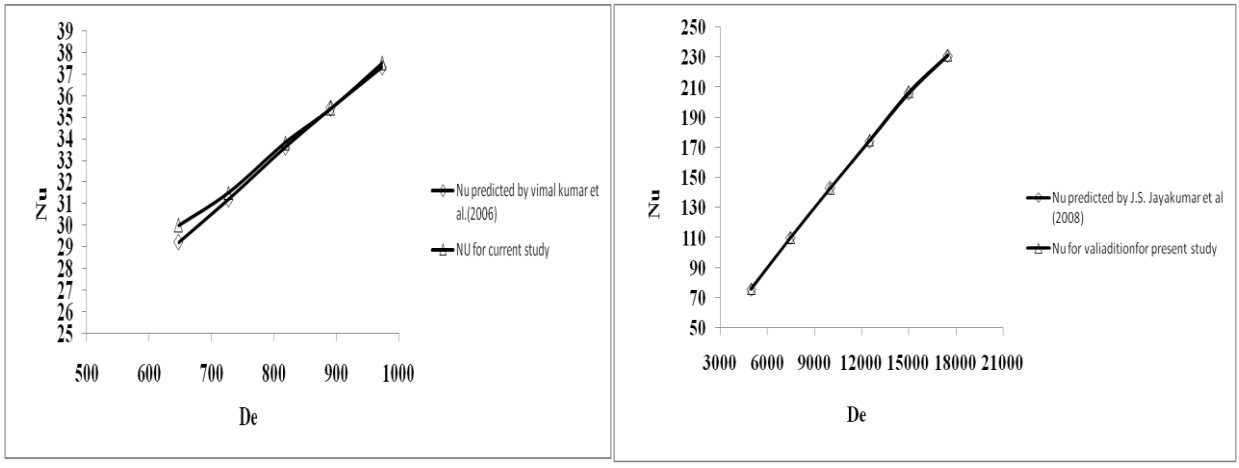

Fig. 5.1 (a) variation of Nu with respect to De predicted by Vimal Kumar et al. (2006) (b) variation of Nu with respect to De predicted by J.S. Jayakumar et al. (2008).

5.2. Constant outer wall temperature

For constant outer wall condition the temperature contour of hot fluid outlet is shown in below fig. 5.2. The inner Nusselt number, friction factor, pumping power are calculated subsequently with respect to Reynolds number.

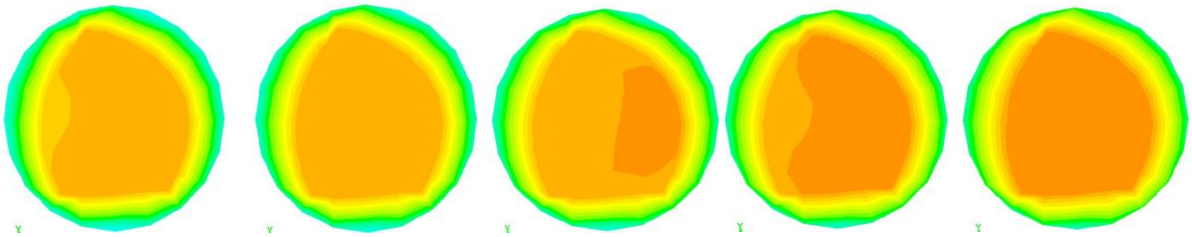

Re=12000 Re=15000 Re=18000 Re=21000 Re=24000

Fig 5.2(a) Temperature contour for D/d=10 at constant wall temperature of 330K

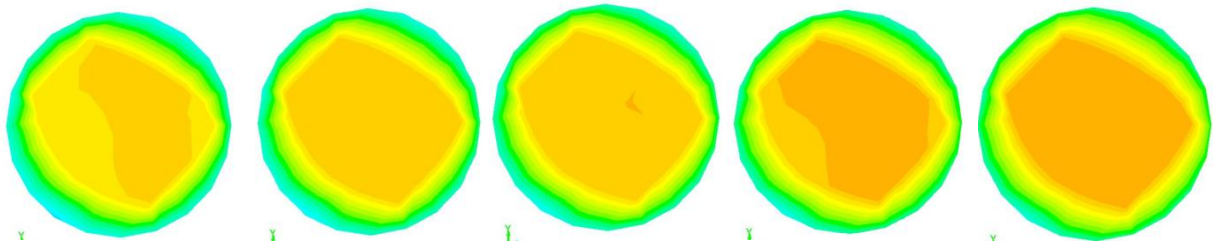

Re=12000 Re=15000 Re=18000 Re=21000 Re=24000

Fig 5.2(b) Temperature contour for D/d=15 at constant wall temperature of 330K

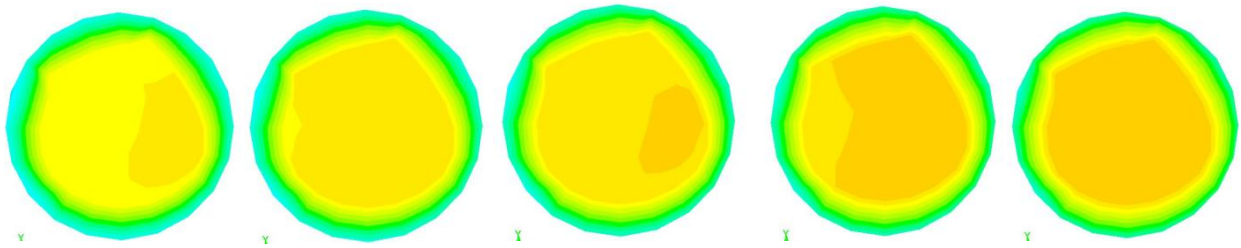

Re=12000 Re=15000 Re=18000 Re=21000 Re=24000

Fig 5.2(c) Temperature contour for D/d=20 at constant wall temperature of 330K

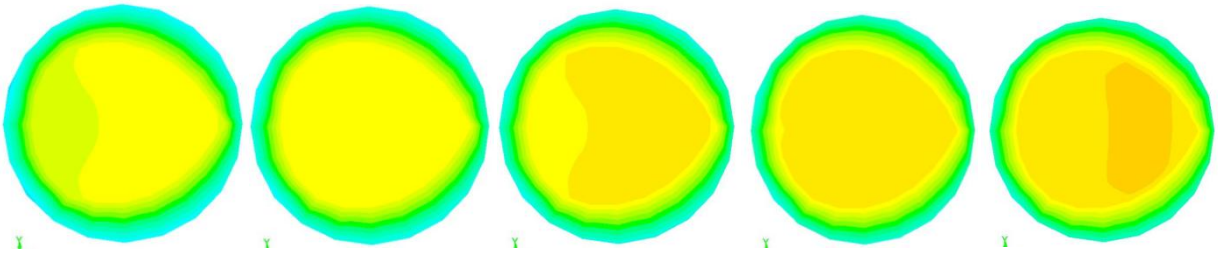

Re=12000 Re=15000 Re=18000 Re=21000 Re=24000

Fig 5.2(d) Temperature contour for D/d=25 at constant wall temperature of 330K

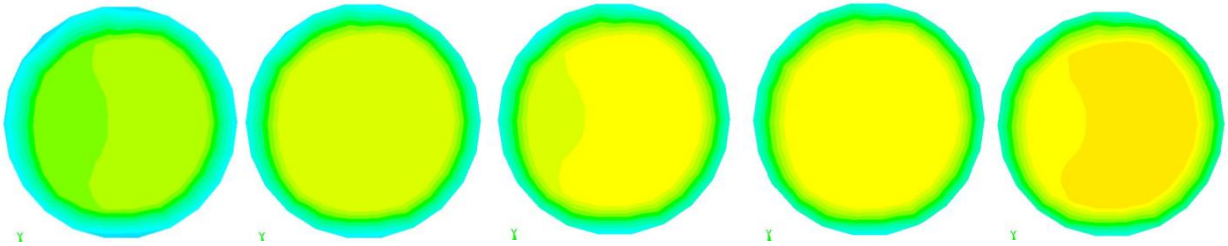

Re=12000 Re=15000 Re=18000 Re=21000 Re=24000

Fig 5.2(e) Temperature contour for D/d=30 at constant wall temperature of 330K

In the above Fig.5.2 temperature contour of outlet of hot fluid for different Reynolds number for constant outer wall temperature of **330K** is shown. In Fig 5.2(a) temperature contour of outlet of hot fluid for D/d=10 shown, where we conclude that with increase in velocity of flow or the Reynolds number, mean temperature at outlet increases. This is because; with increase in Reynolds number velocity of flow increase and with increase in velocity of flow time available for heat transfer between two fluid decreases. We have the flow rate of cold fluid in all case is same but the flow rate of hot fluid increases, so the hot fluid flow past the inner tube with high velocity and not find enough time to transfer heat to the cold fluid. Fig 5.2(b) shows the temperature contour of outlet of hot fluid for D/d=15. By comparing the fig 5.2 (a) and (b) we find that for same Re (for example Re=12000), outlet temperature for D/d=15 is less than outlet temperature for D/d=10. This is due to the reason that with increase in D/d ratio the length of the tube of the exchanger increases, which increases the surface area of contact of heat exchanger. With increase in area of contact the heat transfer rate between two fluid increases. So the outlet temperature of the hot fluid decreases with increases in D/d ratio. It is also shown in the Fig 5.2

(c-e). When the D/d ratio increases from 25 to 30, there is a large decrease in outlet temperature which can be conformed from fig 5.2 (d) and 5.2 (e).

Fig 5.3(a) shows the Nusselt number variation with respect to Reynolds number for different curvature ratio (d/D ratio). It is obvious that with increase in Reynolds number Nusselt number increases. With increases in Reynolds number the flow become more turbulent and mixing of the fluid between two layers occurs more rapidly which will enhance the heat transfer rate. For a particular value of Reynolds number (for example Re=18000or 21000 etc) with decreases in curvature ratio Nusselt number decreases. With decreases in curvature ratio the secondary forces which will act on the fluid element due to flow inside helical tube will decreases.

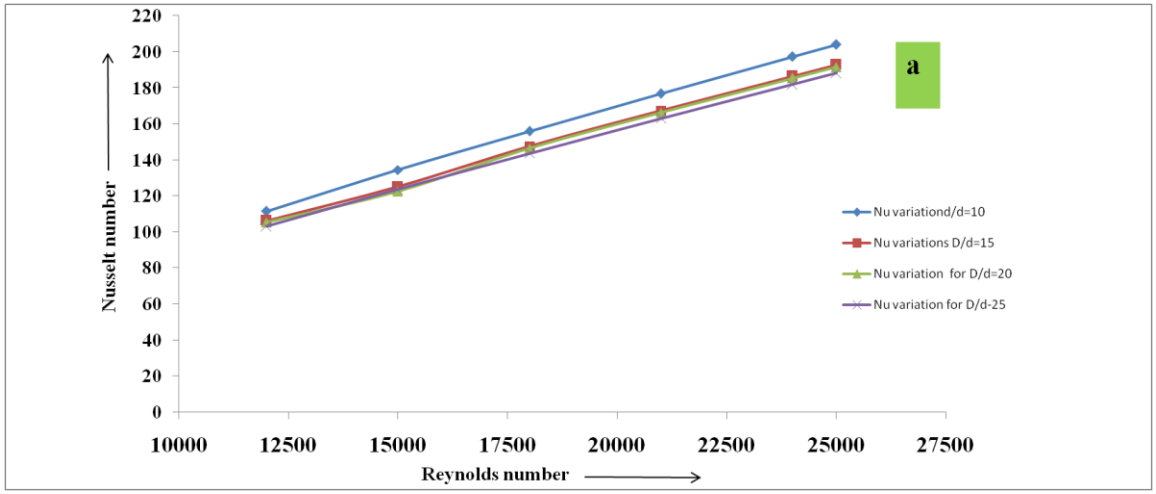

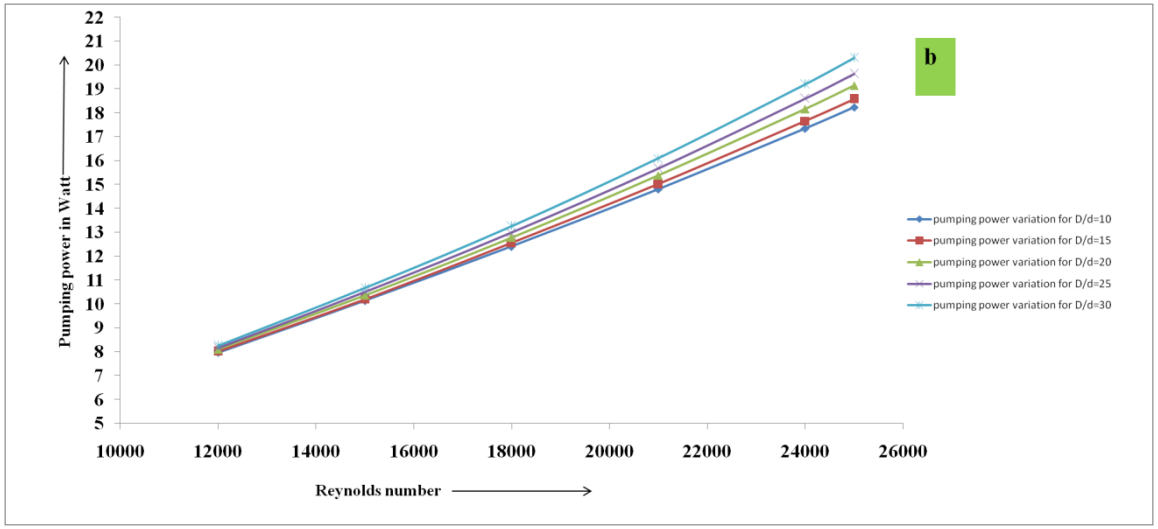

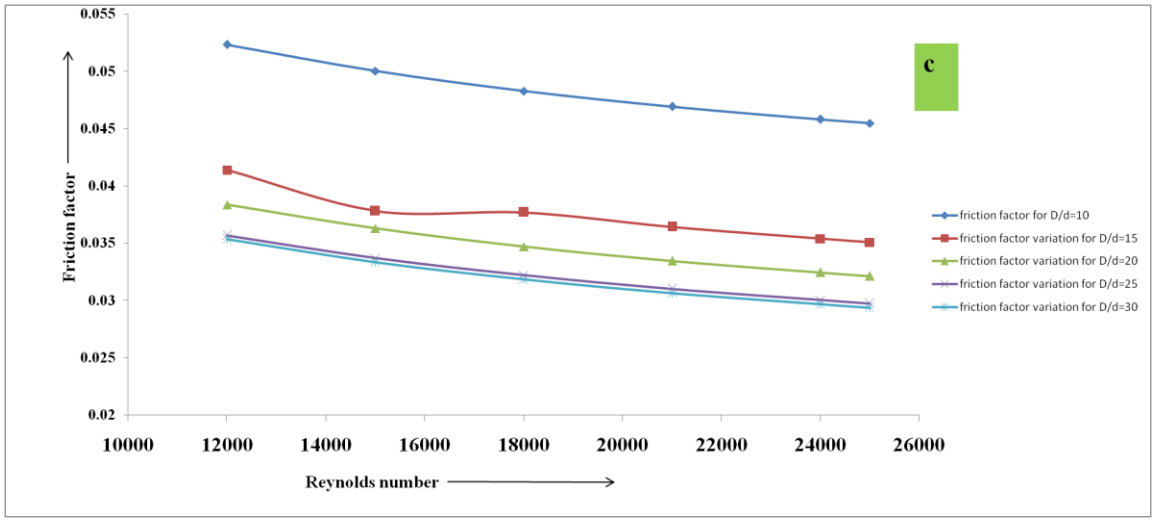

Fig. 5.3 (a) variation of Nu with respect to Re (b) variation of pumping power with respect to Re (c) variation of friction factor(f) with respect to Re for different D/d ratio(inverse of curvature ratio).

Due to decreases in secondary forces the turbulent mixing of fluid will also decreases which will reduces the heat transfer rate or the Nusselt number. As the curvature ratio decreases the variation of Nusselt number for a particular value of Reynolds number is less or insignificant; which can be shown in Fig. 5.3(a).

Fig. 5.3(b) shows the pumping power (Watt) variation with respect to Reynolds number for different D/d ratio. It is shown clearly that with increases in Reynolds number pumping power increases, because with increases in Reynolds number pressure drop between inlet and outlet will increases. With increases in pressure drop more power is required for pumping the fluid. At low Reynolds number variation of pumping power with respect to D/d ratio is in-significant but with increases in Reynolds number pumping power is a strong function of D/d ratio. D/d ratio has maximum effect at Re=25000.

Fig.5.3(c) shows the variation of friction factor with respect to Reynolds number for different D/d ratio. The friction factor will decreases with increases in Reynolds number, which is quite obvious. The variation of friction factor for a particular Reynolds number is maximum between D/d=10 to D/d=15. As we increase the curvature ratio the variation will decreases and it is insignificant between D/d=25 to D/d=30.

Fig.5.4 (a) shows the variation of Nusselt number with respect to D/d ratio (inverse of curvature ratio) for different Reynolds number. As in Fig.5.3 (a) it is explained that with increases in D/d ratio the Nusslet number will decreases. From the graph it is clear that Nusselt number will decreases faster rate when D/d changes from 10 to 15, then between D/d ratios 15 to 20 the change is less. For Re=12000 the percentage change in Nu from D/d ratio 10 to 25 is 7.58% while that for Re=25000, it is 7.8%.

Fig. 5.4(b) shows the variation of pumping power with respect to D/d ratio (inverse of curvature ratio) for different Reynolds number. It can easily understood that with increase in D/d ratio pumping power increase and pumping power is maximum for Reynolds number=25000.

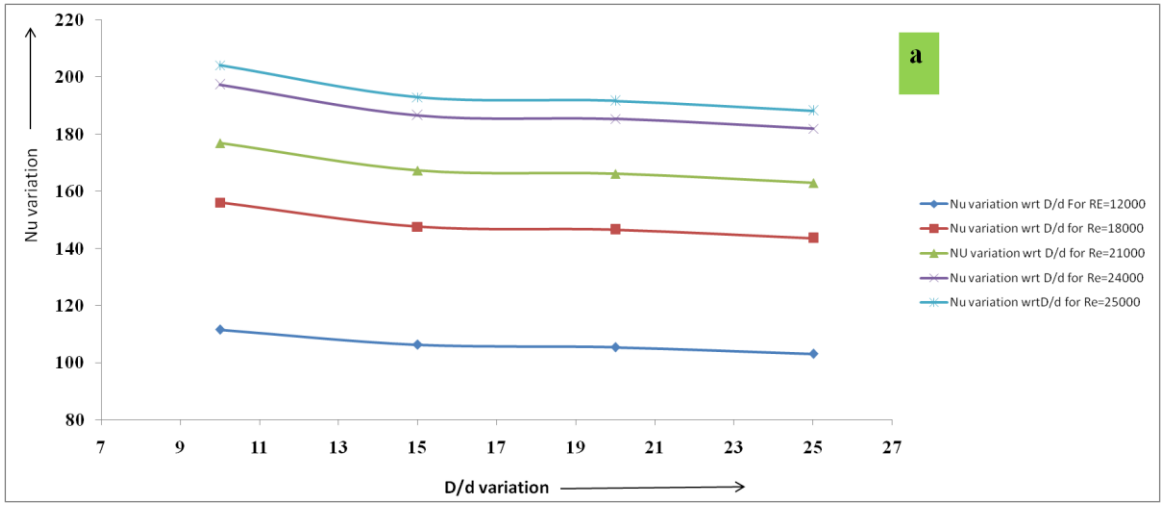

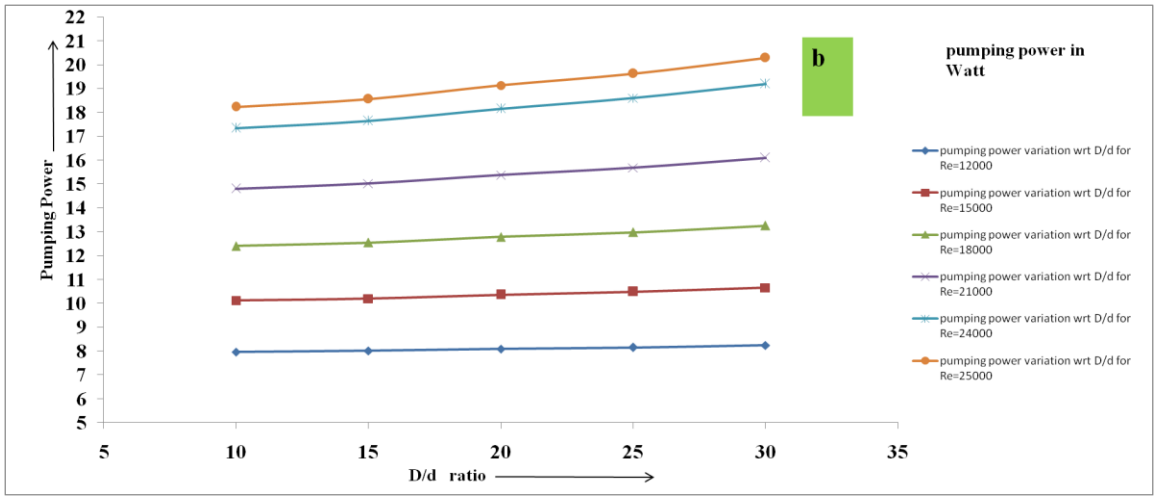

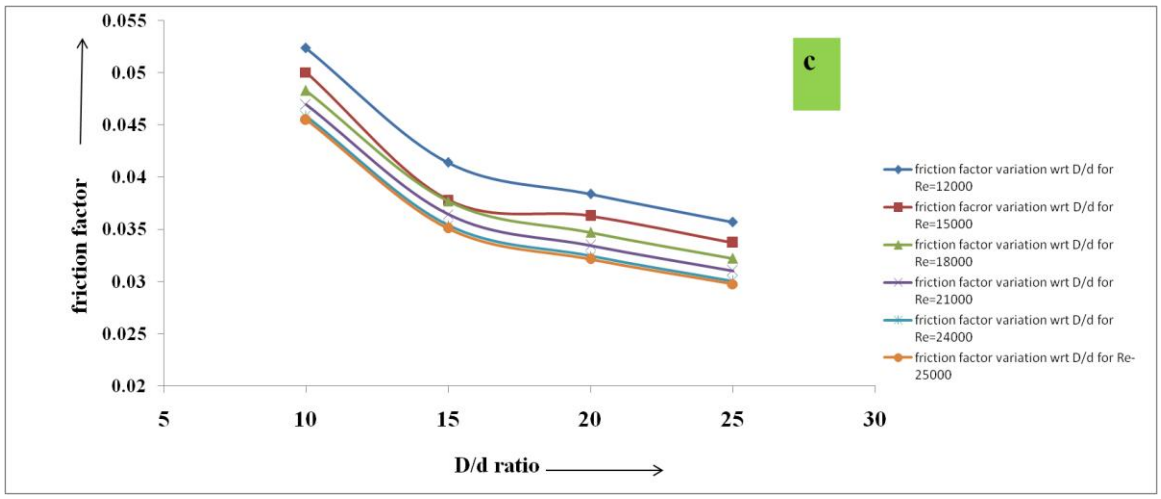

Fig. 5.4 (a) variation of Nu with respect to D/d (b) variation of pumping power with respect to D/d (c) variation of friction factor[f] with respect to Re for different Reynolds number.

With increases in D/d ratio the length of pipe increases and the pressure loss increase which will increase the pumping power requirement.

Fig 5.4 (c) shows the variation between Darcy friction factor with respect to D/d ratio for different Reynolds number. For a particular value of Reynolds number friction factor decreases with decreases in curvature ratio (d/D). For Re=12000 friction factor is maximum and decrease with increase in Re. The change in friction factor is insignificant after Re=24000 for particular D/d ratio which can be understood from the fig 5.4(c). The D/d ratio varying from 10 to 25 percentage decrease in friction factor is 31.84 % for Re=12000.

5.3. Constant outer wall flux condition

This is the general case of heat exchanger which finds applications in furnace where the fluid is

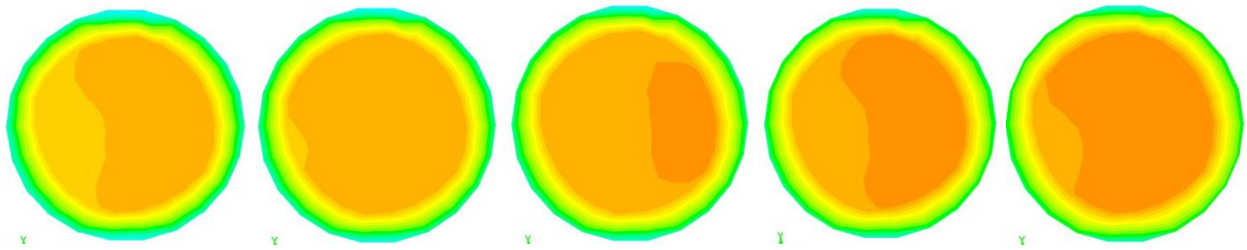

Re=12000 Re=15000 Re=18000 Re=21000 Re=24000

Fig 5.5(a) Temperature contour for D/d=10 at constant heat flux condition

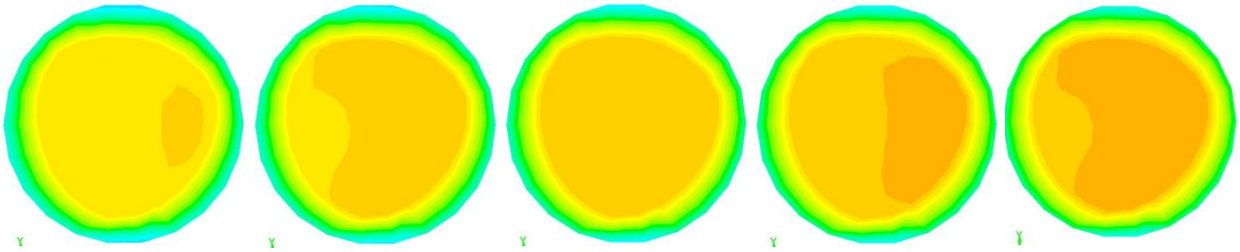

Re=12000 Re=15000 Re=18000 Re=21000 Re=24000

Fig 5.5(b) Temperature contour for D/d=15 at constant heat flux condition

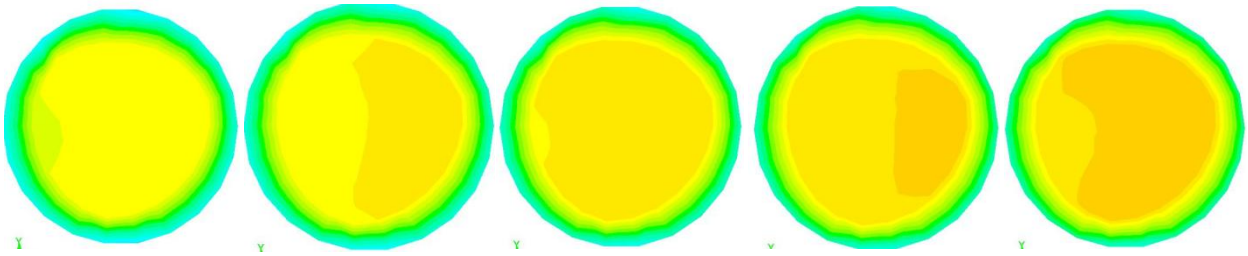

Re=12000 Re=15000 Re=18000 Re=21000 Re=24000

Fig 5.5(c) Temperature contour for D/d=20 at constant heat flux condition

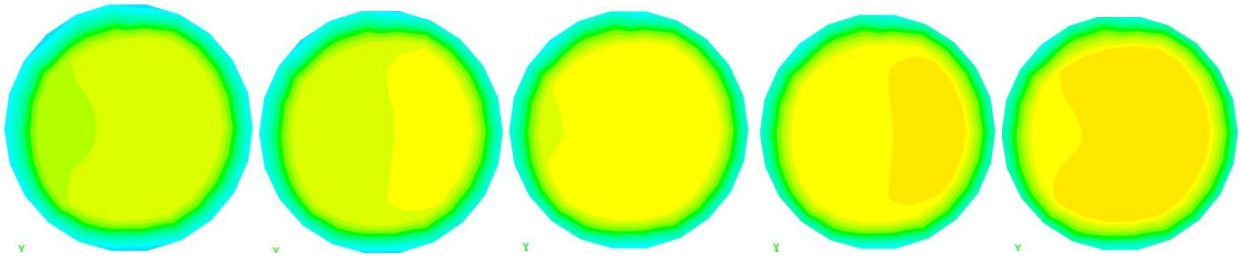

Re=12000 Re=15000 Re=18000 Re=21000 Re=24000

Fig 5.5(d) Temperature contour for D/d=25 at constant heat flux condition

heated from external source with constant heat flux. The water is converted to steam through this type of heat exchangers.

Fig. 5.5 (a-d) shows the temperature contour of hot fluid outlet for different D/d ratio for constant heat flux of 60000W/m^2 at outer wall. As the Reynolds number increases the outlet temperature is more towards the hotter side. While comparing the contours for a particular Reynolds number we find that higher the D/d ratio lower will be the outlet temperature because with increase in D/d ratio the surface area for heat transfer increases. So the outlet temperature

for hot fluid decreases. When we compare the contours for constant wall conditions (Fig.5.3) with constant heat flux conditions (Fig.5.5) at the outer wall for a particular D/d ratio and Reynolds number; constant wall temperature has lower outlet temperature compared to constant heat flux condition at the outer wall.

Fig. 5.6 (a) shows the variation of Nusselt number with respect to Reynolds number for different D/d ratio (inverse of curvature ratio). In this Fig. 5.6(a), Nu is taken in Y-axis and Re in X axis keeping D/d ratio constant. Then the D/d ratio varied from 10 to 30 with an interval of 5 and Nusselt number variation with respect to Reynolds number was drawn in the figure. It is obvious that with increases in Reynolds number the Nusselt number increases because with increases in flow rates the turbulence between the fluid elements increases. The Nusselt number

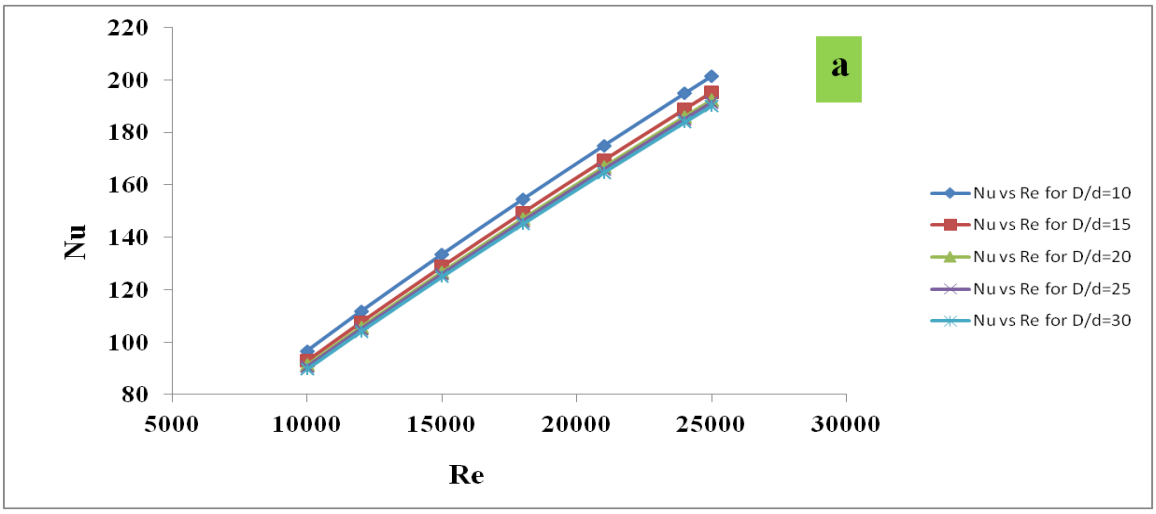

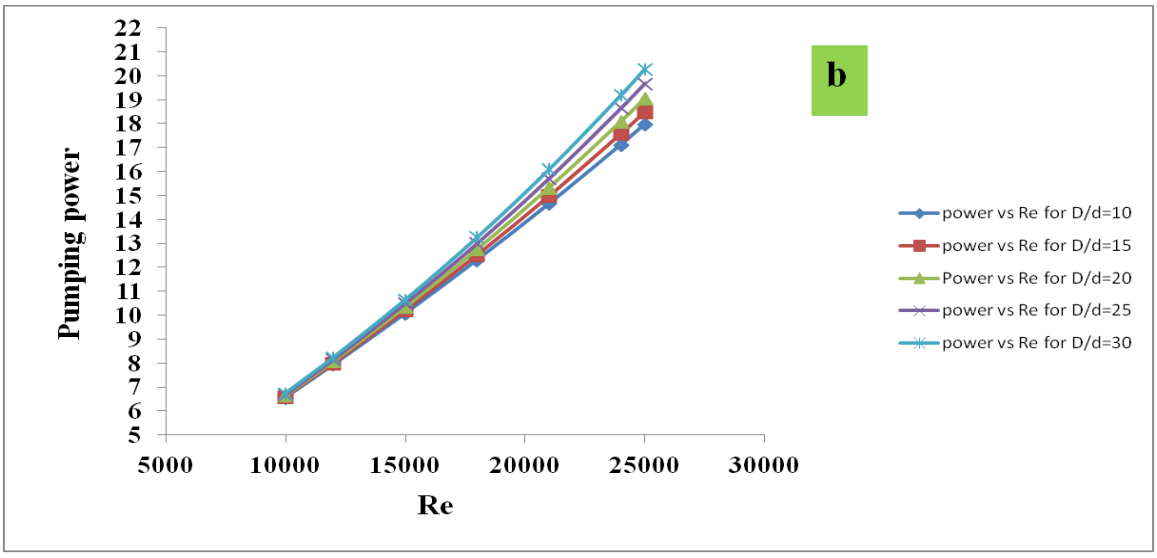

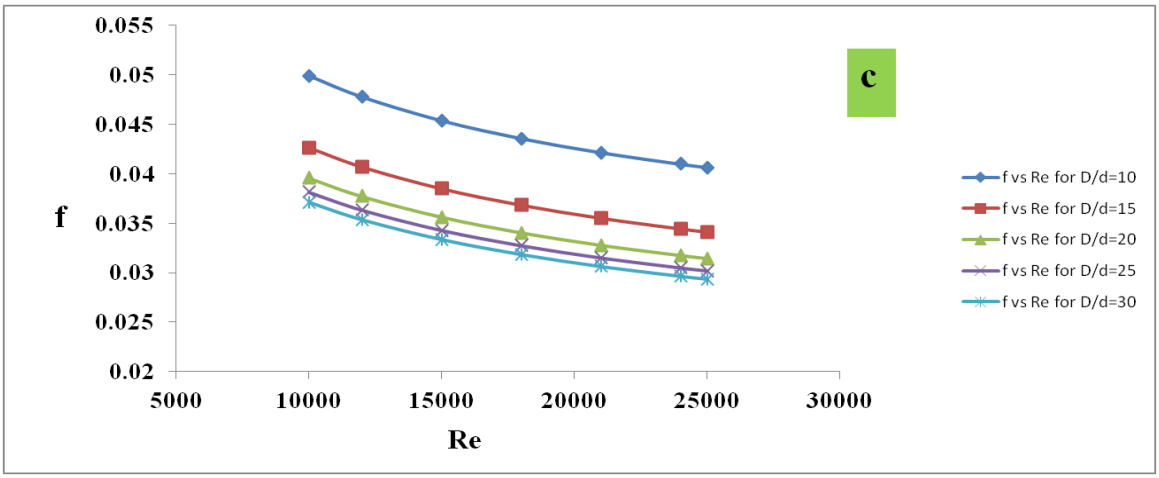

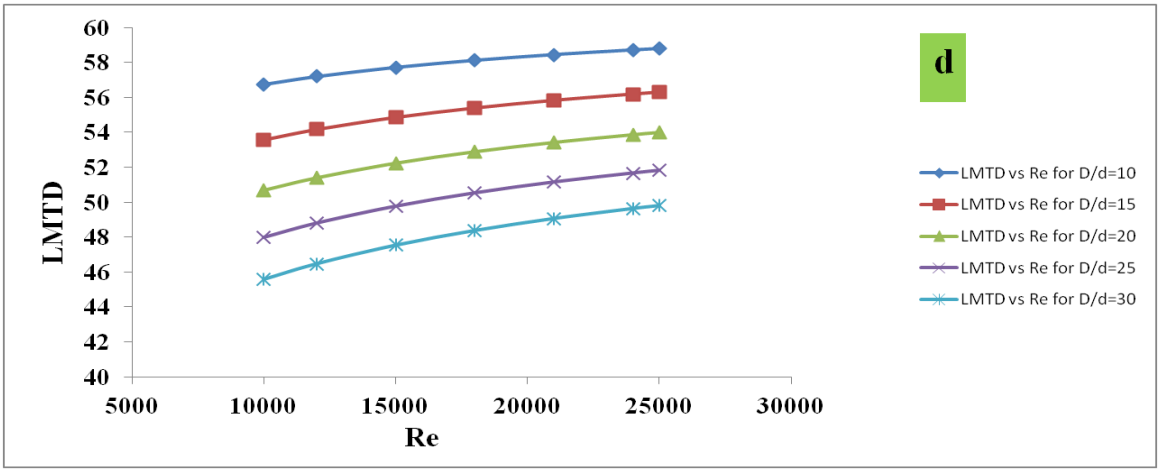

Fig 5.6 (a) variation of Nu with respect to Re (b) variation of pumping power with respect to Re (c) variation of friction factor with respect to Re (d) variation of LMTD with respect to Re for different D/d ratio for constant heat flux at outer wall condition.

is maximum for all value of Reynolds number for D/d=10 and it is decreases with increases in D/d ratio. The variation of Nusselt number with respect to Reynolds number between D/d=25 and D/d=30 is very less and with further increases in D/d ratio, the variation almost vanishes.

Fig. 5.6(b) shows the variation of pumping power (Watt) with respect to Reynolds number for different D/d ratio (inverse of curvature ratio). Pumping Power is taken in Y-axis and Reynolds number in X-axis for a constant D/d ratio then the D/d ratio varies to get series of line showing the variation. However, the pumping power is a strong function of pressure drop and flow velocity. So with increases in flow velocity pressure drop increases and with increases in pressure drop the power required for pumping the fluid increases.

Fig 5.6 (c) shows the variation between Darcy friction factor with respect to Reynolds number for different D/d ratio. In Y-axis friction factor is taken and in X-axis Reynolds number was taken for a particular value of D/d ratio. We know that the friction factor in turbulent condition was a strong function Reynolds number and relative roughness of pipe surface. The friction factor is inversely proportional to the Reynolds number. With increase in Reynolds number friction factor decreases. With increase in D/d ratio the surface area increases and the relative roughness also increases and in that condition roughness predominate the Reynolds number.

Fig 5.6 (d) shows the variation between Log mean temperature differences with respect to Reynolds number for different D/d ratio. With increases in Reynolds number the LMTD increases. We know that larger the LMTD; lager will be the temperature driving force, which will increases the heat transfer. For D/d=10 has maximum LMTD for all case of Reynolds number. The increases in value of log mean temperature difference with respect to Reynolds number is due to less time of contact with in the heat exchanger.

5.4. Insulated outer wall condition:

This is the general case of heat exchanger where the main aim is to transfer the heat between two fluids which are maintained at different temperature. We find applications of this type of heat exchangers in air conditioning plant, food storage, auto mobile industries and research lab.

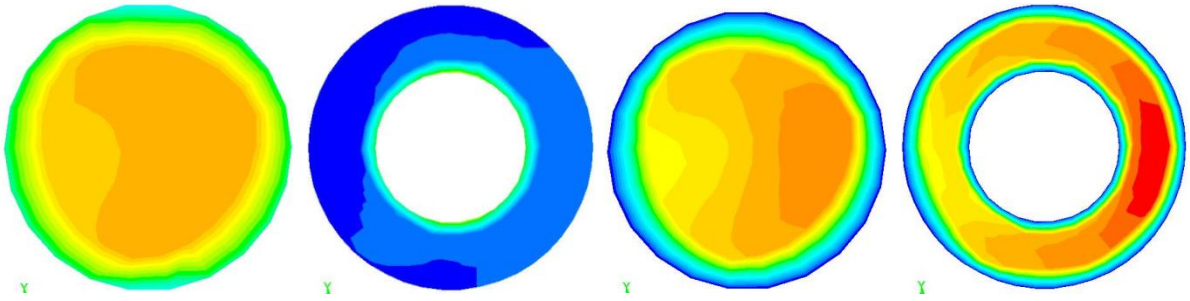

(a) **(b)** **(c)** **(d)**

Fig 5.7 (a) outlet temperature contour of hot fluid (b) outlet temperature contour of cold fluid (c) velocity contour of hot fluid outlet (d) velocity contour of cold fluid outlet

Fig. 5.7 shows the temperature and velocity contour of hot fluid outlet and cold fluid outlet for D/d=15 at Reynolds number 24000. The Fig.5.7 (a) shows the temperature contour of hot fluid at outlet. The temperature decreases from center towards wall of inner tube. For outer tube (fig.5.7(b)), it is maximum at the center of annulus and decreases toward the outer wall. Fig.5.7(c-d) shows the velocity contour of hot and cold fluid and the velocity is minimum at the wall and maximum at the center.

Fig. 5.8 (a) shows the variation of Nusselt number with respect to Reynolds number for different D/d ratio. In this Fig. 5.8(a), Nu is taken in Y-axis and Re in X axis keeping D/d ratio constant. Then the D/d ratio varied from 10 to 30 with an interval of 5 and Nusselt number variation with respect to Reynolds number was drawn in the figure. With increases in Reynolds number the Nusselt number increases because with increases in flow rates the turbulence between the fluid elements increases. Due to flow past the helical tube there is strong a centrifugal force acting on fluid element which will enhance the heat transfer rate.

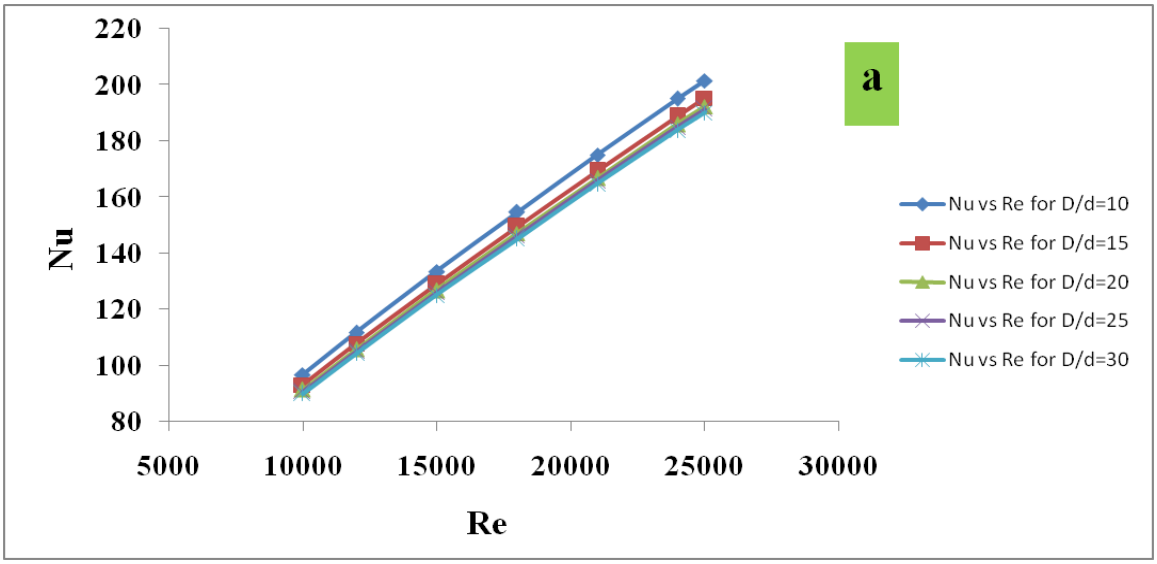

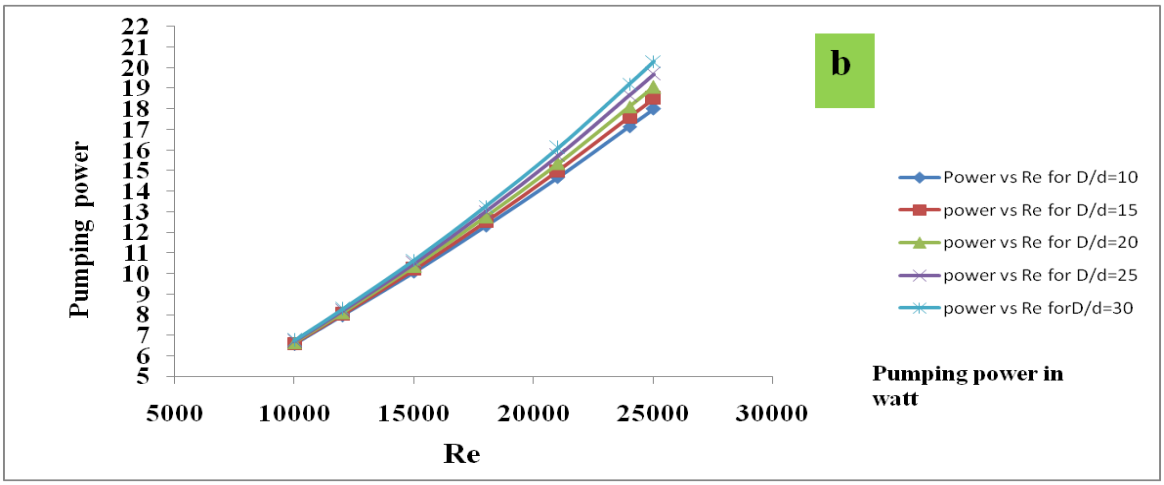

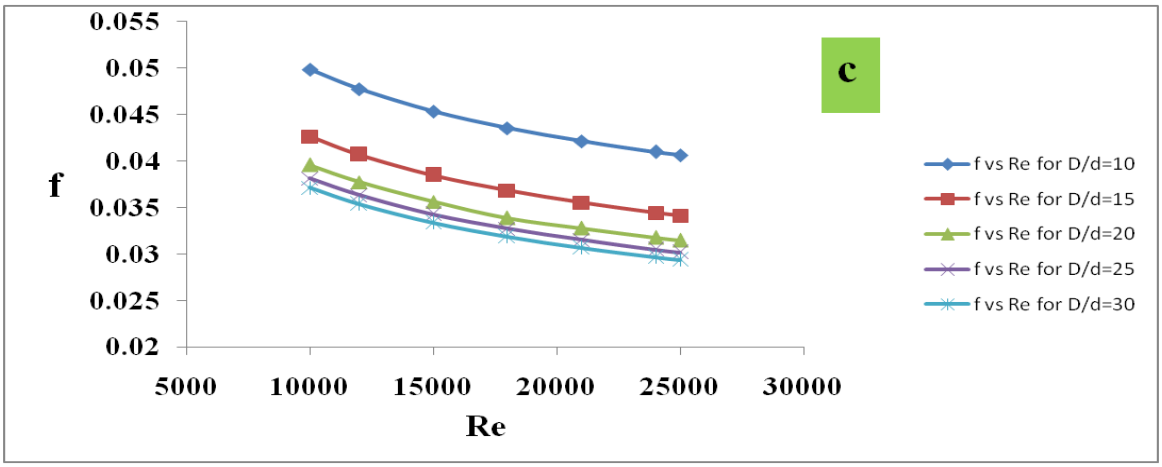

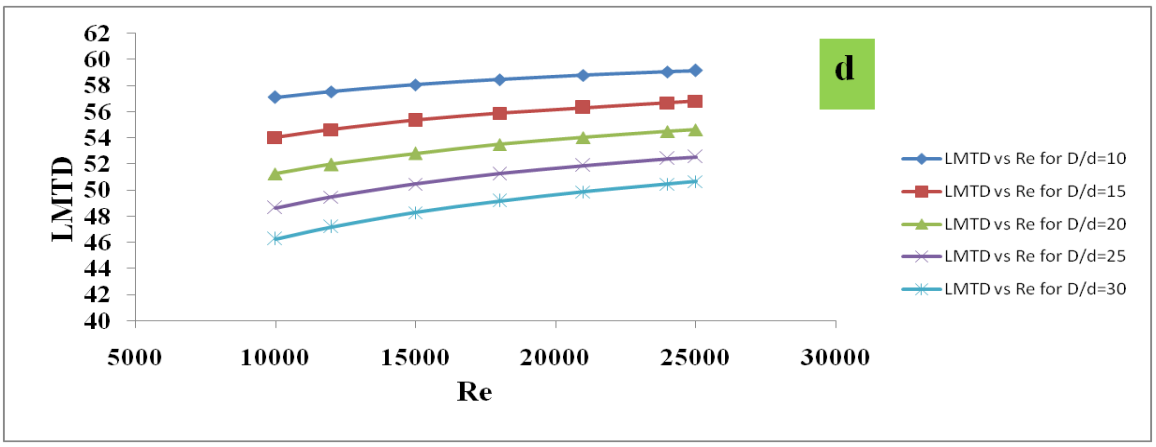

Fig 5.8 (a) variation of Nu with respect to Re (b) variation of pumping power with respect to Re (c) variation of friction factor with respect to Re (d) variation of LMTD with respect to Re for different D/d ratio for insulated outer wall condition.

Fig. 5.8 (b) shows the variation of pumping power (Watt) with respect to Reynolds number for different D/d ratio (inverse of curvature ratio). Pumping Power is taken in Y-axis and Reynolds number in X-axis for a constant D/d ratio. Then the D/d ratio varies to get series of lines showing the variation of power requirement. The change in pumping power is due to the pressure drop and the change in the pressure drop with Reynolds number is due to the increasing contraction and expansion pressure losses at the inlet and outlet portion of the helical coil heat exchanger.

Fig 5.8 (c) shows the variation between Darcy friction factor with respect to Reynolds number for different D/d ratio. In Y-axis friction factor is taken and in X-axis Reynolds number was taken for a particular value of D/d ratio. The decreases in friction factor from Re=10000 to Re=25000 for D/d=10 is 18.50%. Similarly for D/d=30 the decrease in friction factor is almost 20.90%.

Fig 5.8 (d) shows the variation between Log mean temperature differences with respect to Reynolds number for different D/d ratio. LMTD is calculated for inlet and outlet of hot and cold fluid and drawn on Y axis and similarly the Reynolds number on X axis, in Fig.5.8 (d). The value of LMTD increases with increases with Reynolds number.

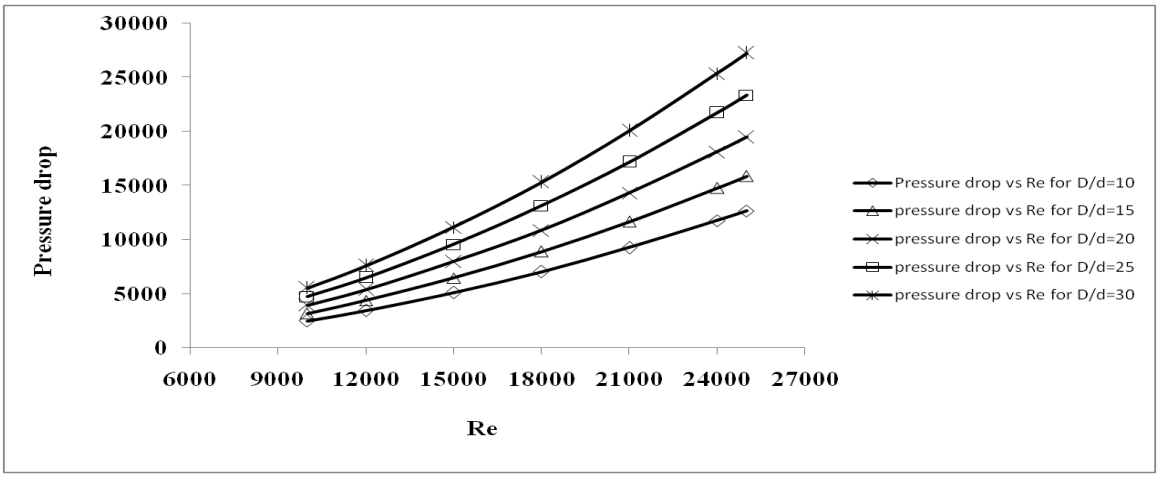

Fig. 5.9 pressure drop variation with respect to Re for insulated condition

In above Fig. 5.9 pressure drop variation with respect to Reynolds number is shown for outer wall insulated condition. The pressure drop variation is in Pascal unit. With increases in Reynolds number the pressure drop increases. When the flow is more turbulent more amount of

energy is lost due to conversion pressure energy to kinetic energy. With increases in D/d ratio the pressure loss increases, because with increase in D/d ratio the length of the pipe increases and with increase in length of pipe the loss is more.

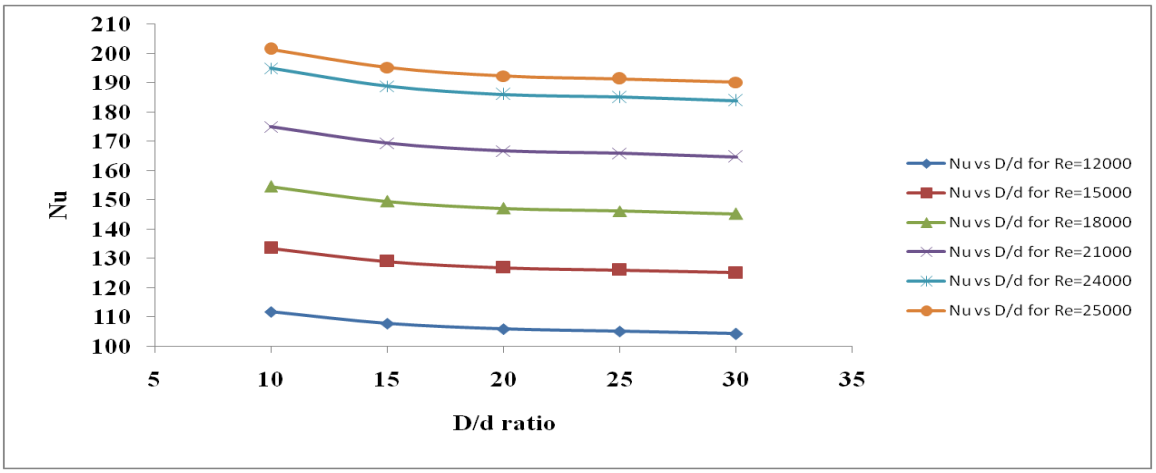

Fig. 5.10 (a) variation of Nu with respect to D/d ratio for different Re

Fig.5.10 (a) shows the variation of Nusselt number with respect to D/d ratio for different Reynolds number. As in Fig.5.9 (a) it is explained that with increases in D/d ratio the Nusslet number will decreases. From the graph it is clear that Nusselt number will decreases when D/d changes from 10 to 15, then for 15 to 20 the change is less and it gradually decreases with further increase in D/d ratio because turbulence due to curvature effect disappear and flow through coiled tube changed to flow through a straight tube.

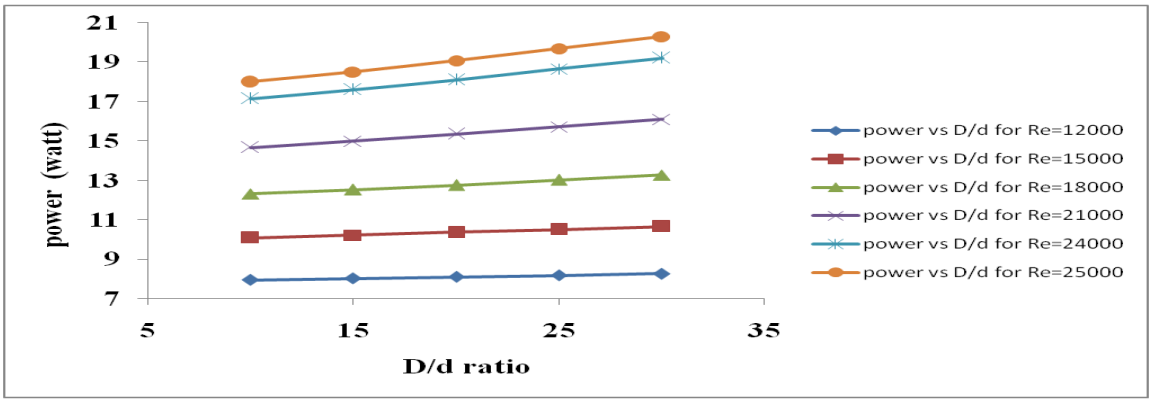

Fig. 5.10 (b) variation of pumping power with respect to D/d ratio for different Re

Fig. 5.10(b) shows the variation of pumping power with respect to D/d ratio for different Reynolds number. It can easily understood that with increase in D/d ratio pumping power increase and pumping power is maximum for Reynolds number=25000. With increases in D/d ratio the length of pipe increases and the pressure loss increase which will increase the pumping power requirement. Also with increase in Reynolds number the turbulent flow will increase which will increases the pressure loss and ultimately the power requirement.

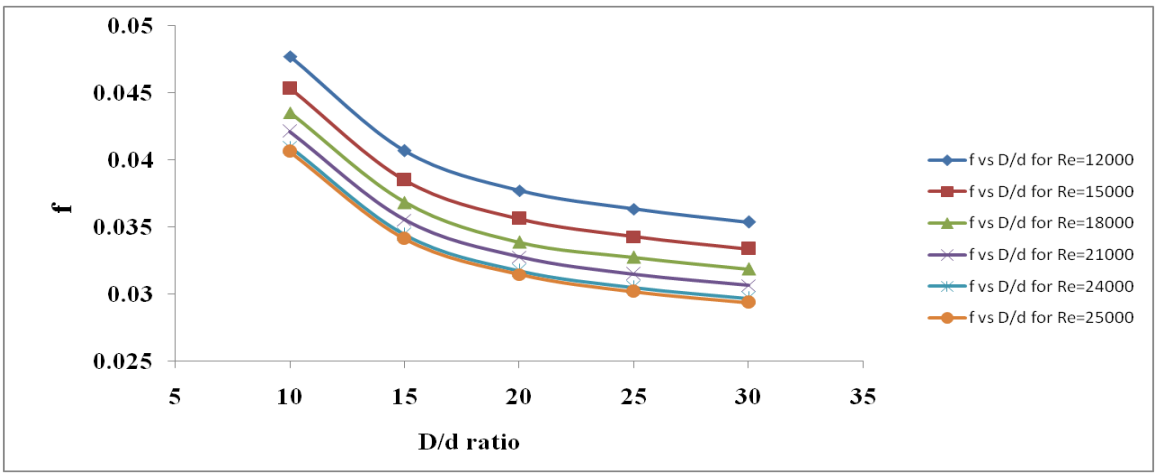

Fig. 5.10 (c) variation of friction factor[f] with respect to D/d ratio for different Re

Fig 5.10 (c) shows the variation between Darcy friction factor with respect to D/d ratio for different Reynolds number at insulated outer wall condition. For a particular value of Reynolds number friction factor decreases with increase in D/d ratio. For Re=12000 friction factor is maximum and decrease with increase in Re. The decrease in friction factor is more for D/d ratio varying from 10 to 15 and it decreases with further increase in D/d ratio.

Fig 5.10 (d) shows the variation between LMTD with respect to D/d ratio for different Reynolds number at insulated outer wall condition. For a particular value of Reynolds number LMTD decreases with increase in D/d ratio. For Re=25000 LMTD is maximum and decrease with decrease in Re. For D/d ratio varying from 10 to 30 the percentage decrease in LMTD is 18.003% for Re=12000. For Re=25000 the percentage decrease in LMTD is 14.3%.

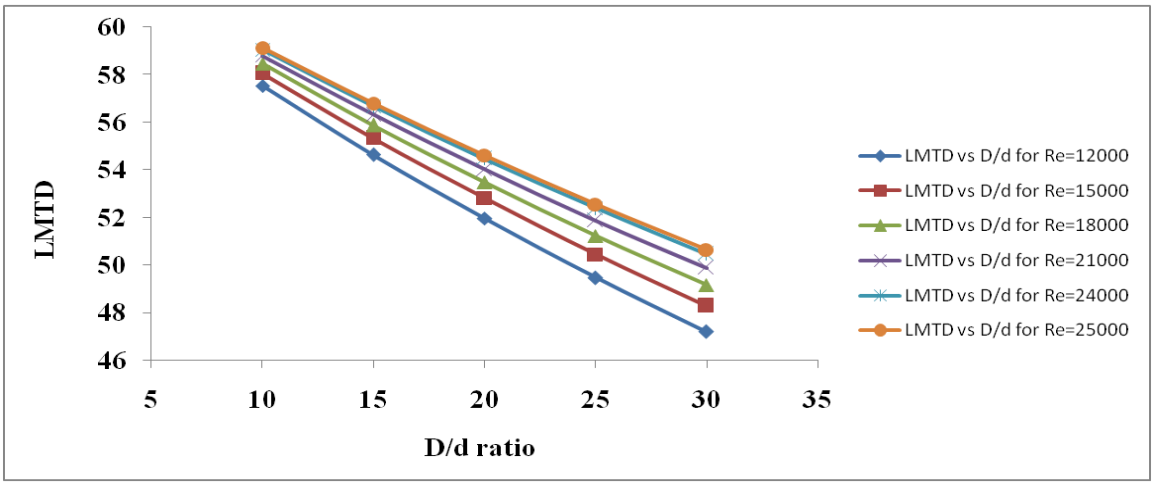

Fig. 5.10 (d) variation of LMTD with respect to D/d ratio for different Re

5.5. Convective heat transfer at the outer wall

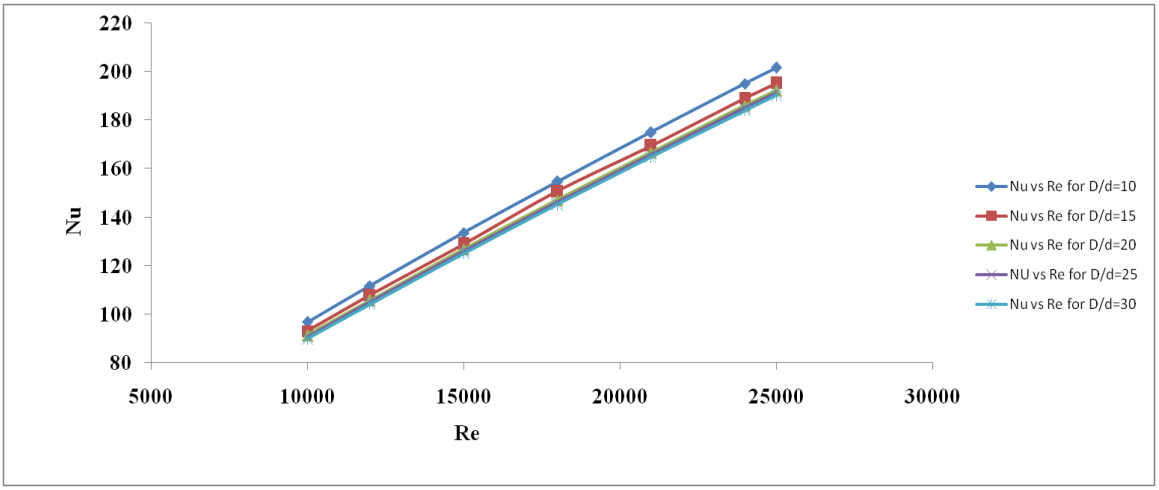

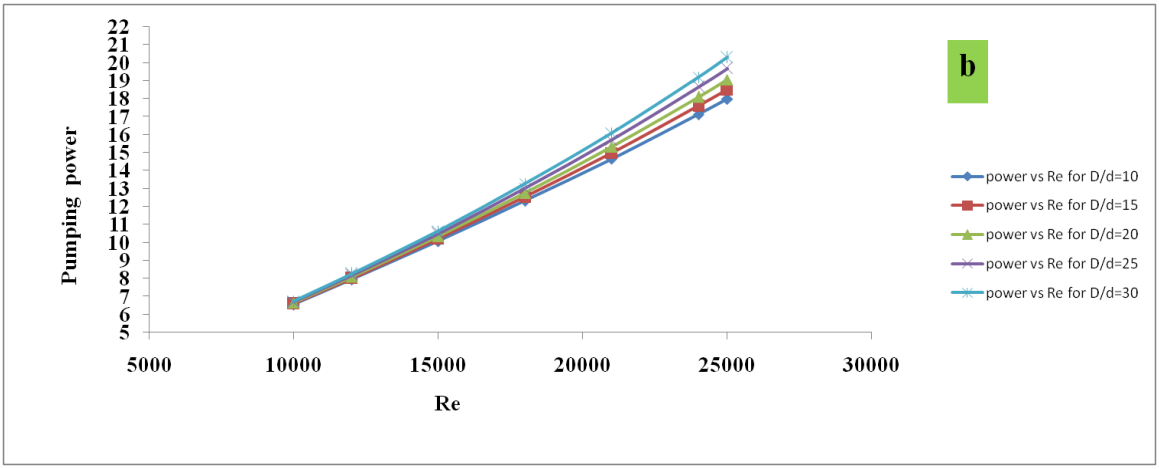

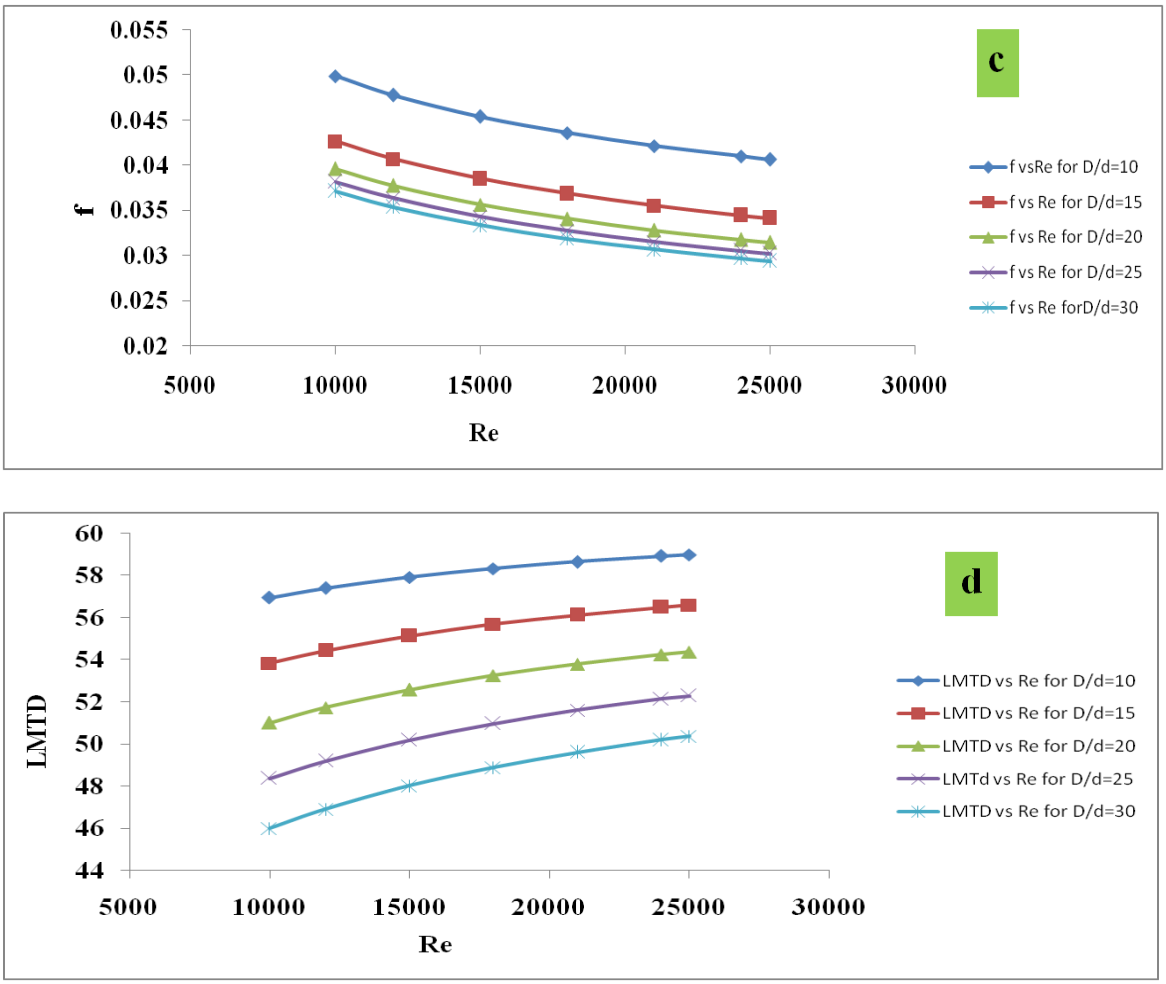

Fig 5.11 (a) variation of Nu with respect to Re (b) variation of pumping power with respect to Re (c) variation of friction factor with respect to Re (d) variation of LMTD with respect to Re for different D/d ratio for convective heat transfer condition at outer wall.

We find applications of this type of heat exchangers in air conditioning plant, boiler and furnace of power plants and automobile industries. Fig. 5.11 (a) shows the variation of Nusselt number with respect to Reynolds number for different D/d ratio. In this Fig. 5.11(a), Nu is taken in Y-axis and Re in X axis keeping D/d ratio constant. Here the outer wall was taken convective heat transfer with heat transfer coefficient of 4000W/m^2 and outlet fluid temperature of 300K. Similar type of variation can be observed between Nu and Re as explained above. As the inner Nusselt number is the function Reynolds number which is a function of velocity at inlet. There is no change in wall property occurred at the inner tube and it is independent of the boundary

condition of outer wall of outer tube. So for all the four cases discussed so far give same inner Nusselt number.

Fig. 5.11 (b) shows the variation of pumping power (Watt) with respect to Reynolds number for different D/d ratio. Here the outer wall was taken convective heat transfer with heat transfer coefficient of 4000W/m^2 and outlet fluid temperature of 300K. Similar type of variation can be observed between pumping power requirement and Re for different D/d ratio as explained above.

Fig 5.11 (c) shows the variation between Darcy friction factor with respect to Reynolds number for different D/d ratio and Fig 5.10 (d) shows the variation between Log mean temperature differences with respect to Reynolds number for different D/d ratio for outer wall convective heat transfer coefficient.

5.6. Variation of thermal properties with respect to different boundary conditions:

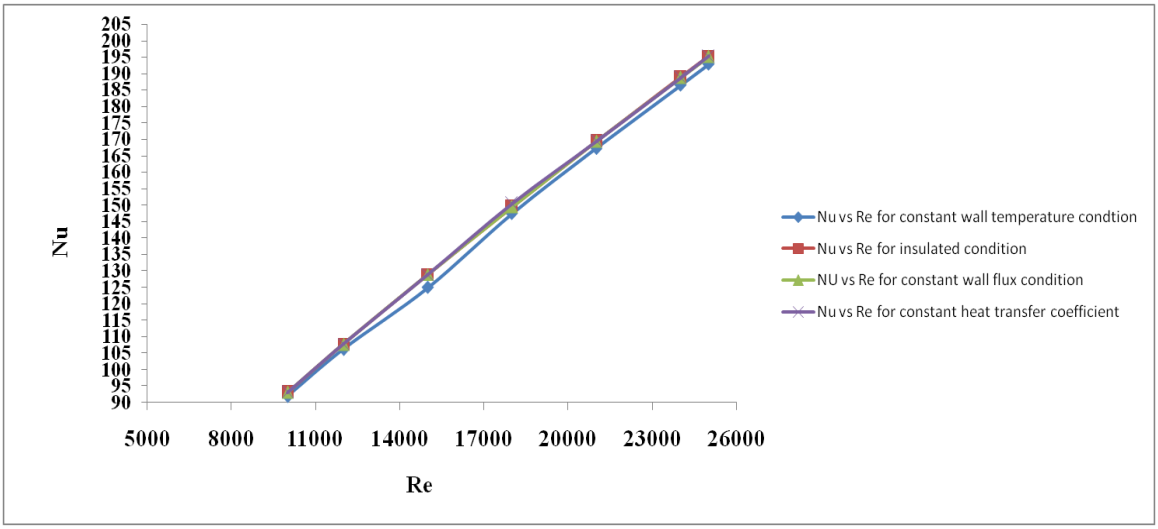

Fig 5.12 (a) variation of Nu with respect to Re for different boundary conditions

In Fig. 5.12 (a) shows the variation of inner Nusselt number with respect to Reynolds number for different boundary conditions. The D/d ratio for this graph is 15 and is remain constant. There is no significant deviation between the Nusselt number is observed for different boundary conditions. The deviation is insignificant because the inner Nusselt number is function of inlet velocity of hot fluid and the inner wall boundary condition which is coupled in all the

cases. As we change the outer wall boundary condition of outer tube, the outer fluid Nusselt number may changes. But the higher mass flow rate of outer fluid does not allow the outer boundary condition to affect the inner Nusselt number.

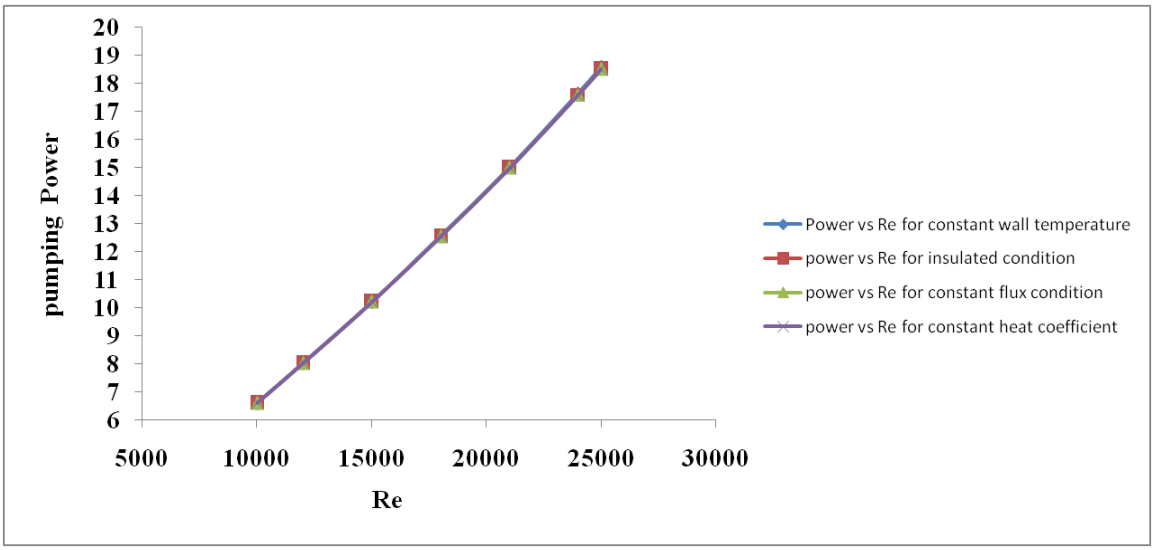

Fig 5.12 (b) variation of Pumping power with respect to Re for different boundary conditions

In Fig. 5.12 (b) shows the variation of pumping power of hot fluid with respect to Reynolds number for different boundary conditions. The D/d ratio for this graph is 15. We know that pumping power is the function of volume flow rate and the pressure drop. With increase in Reynolds number volume flow rate and pressure drop increases which will increase power requirement. But for different outer wall boundary conditions the pumping power remains constant because volume flow rate and pressure drop of hot fluid does not change and is independent of outer boundary conditions or the outer boundary condition is insufficient to produce the change in inner fluid condition.

In Fig. 5.12 (c) shows the variation of Darcy friction factor of hot fluid with respect to Reynolds number for different boundary conditions. The D/d ratio for this graph is 15. From the graph it is clear that except constant wall temperature the all other boundary condition gives same results.

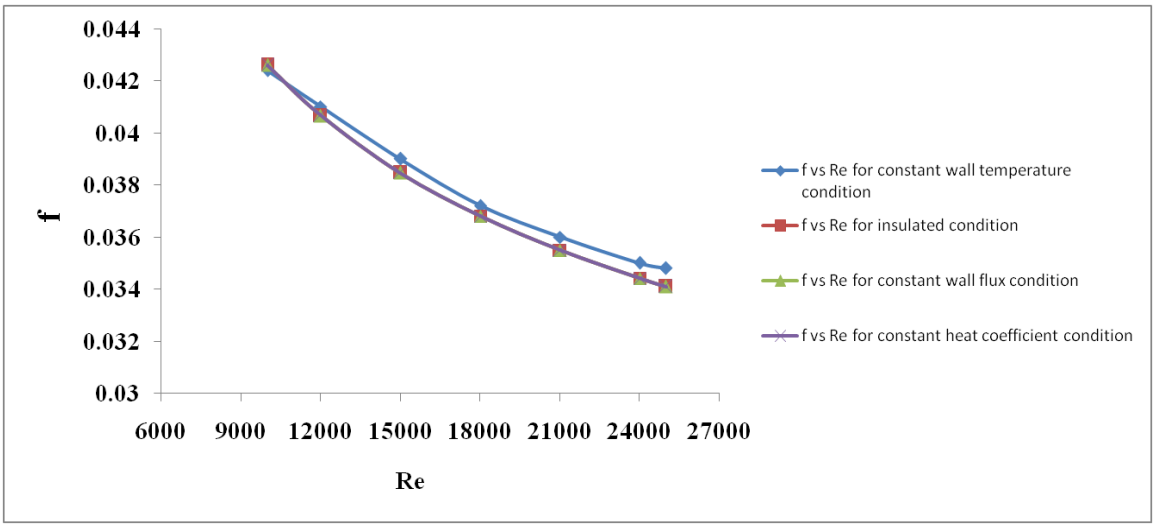

Fig 5.12 (c) variation of friction factor with respect to Re for different boundary conditions

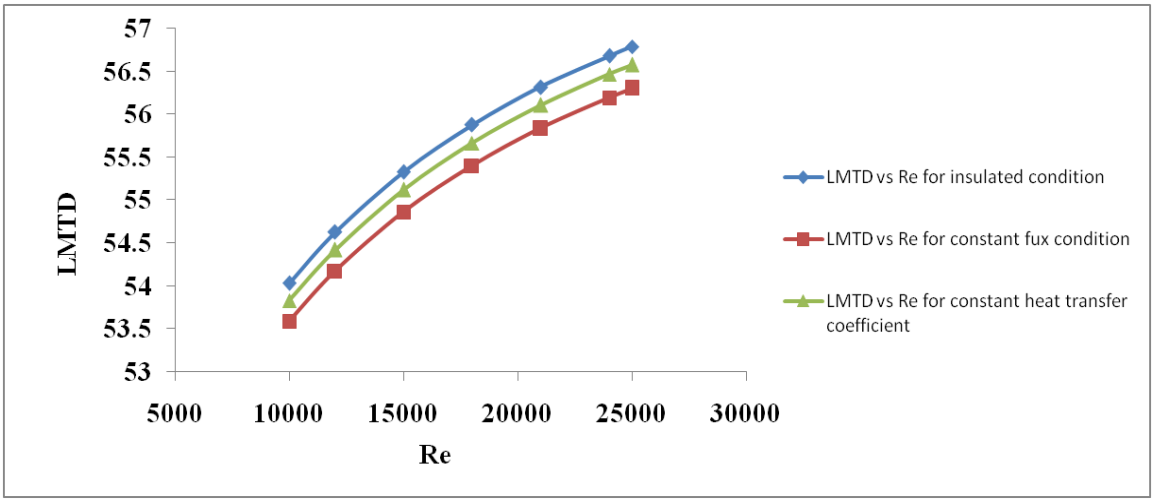

Fig 5.12 (d) variation of LMTD with respect to Re for different boundary conditions

In Fig. 5.12 (d) shows the variation of Log mean temperature difference with respect to Reynolds number for different boundary conditions. The D/d ratio for this graph is 15. From the graph it is clear that LMTD changes for different boundary conditions. As the outer wall of outer fluid (cold fluid) is subjected to different boundary condition its outlet temperature changes accordingly. We know that the LMTD depends on both inlet and outlet of hot and cold fluid and with change in outlet temperature of both hot and cold fluid it will change. For insulated outer wall condition LMTD is maximum indicating maximum driving force for heat transfer compared to other boundary conditions.

5.7. Optimization of the heat exchanger for different d/d condition

Improving the heat transfer rate and at the same time reducing the pumping powers are the key factors while designing a heat exchanger. To increase the heat transfer rate the Nusselt number should be high as possible. But with increases in Reynolds number the flow become more turbulent and it increases the pressure drop across the heat exchanger. If more is the pressure loss more will be the pumping power required. With increases in pumping power the cost of the exchanger increase. So we have to make a compromise between increase in heat transfer rate with increase in pumping power requirement.

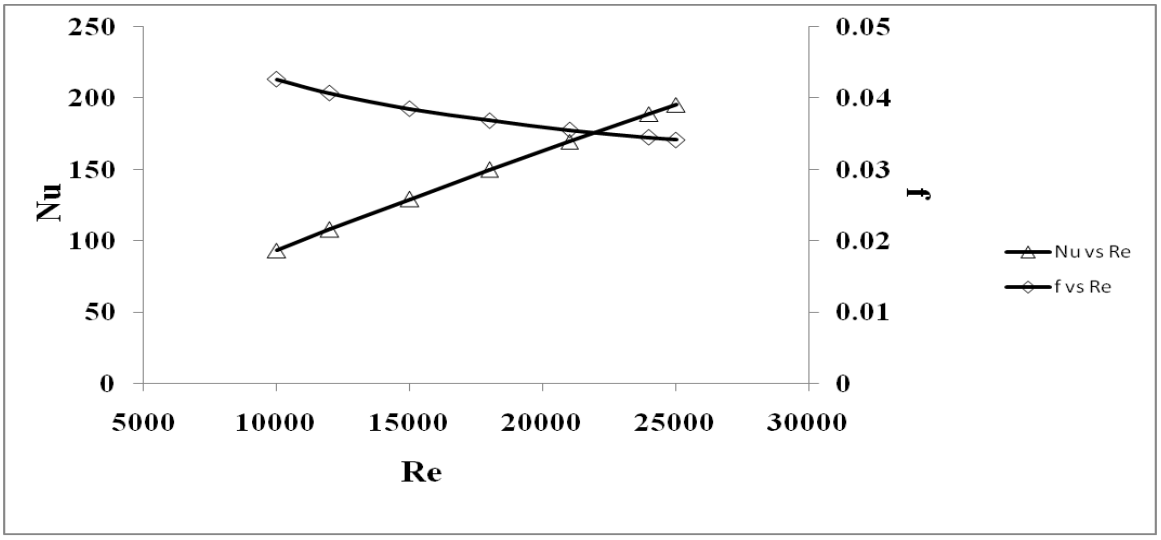

Fig. 5.13 (a) variation of Nu and f with respect to Re for D/d=15

Fig .5.13 (a) shows the variation of Re with Nu and also between Re and friction factor (f) for D/d=15. The optimize condition was considered for insulated outer wall condition. The Nusselt number variation is taken in primary Y-axis and friction factor in secondary Y-axis. With increase in Reynolds number Nusselt number increases and friction factor decreases. Both these curve intersect each other at Re=22000. This intersection point is the optimize condition because with further increase in Re power required increases at a higher rate than that of the Nusselt number. So it is uneconomical to increase the Re beyond this range.

Fig .5.13 (b) shows the variation of Re with Nu and also between Re and f for D/d=20. The optimize condition was considered for insulated outer wall condition. The Nusselt number variation is taken in primary Y-axis and friction factor in secondary Y-axis. The optimize

condition occur almost at Re=20500. By comparing Fig. 5.10(a) and 5.10 (b) we find that with less Reynolds number we achieved the optimize condition.

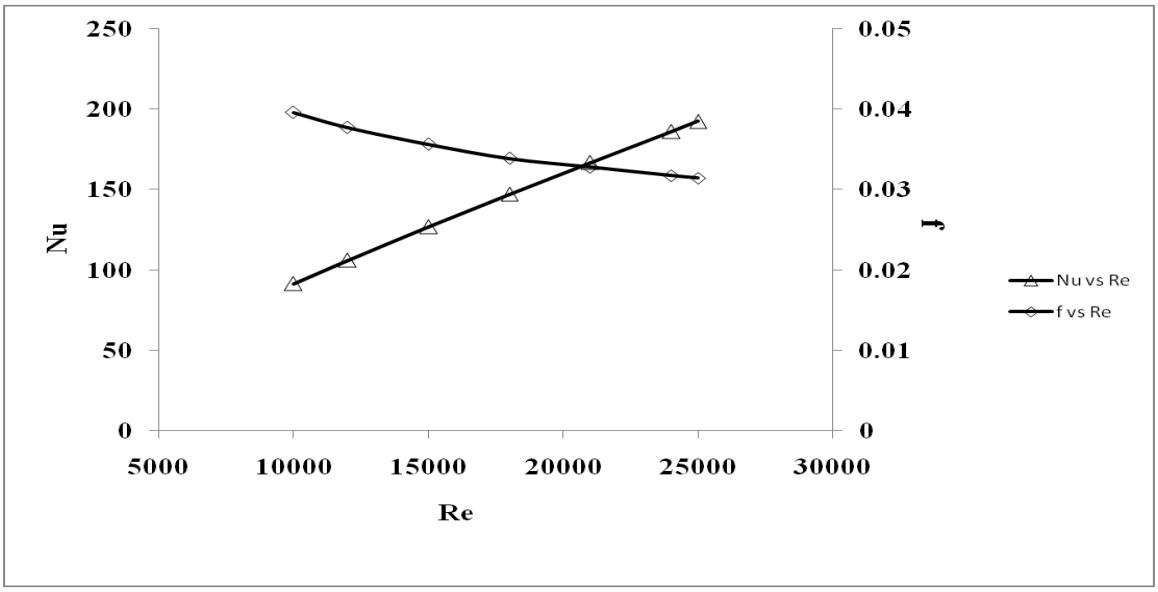

Fig. 5.13 (b) variation of Nu and f with respect to Re for D/d=20

Fig .5.13 (c) shows the variation of Re with Nu and also between Re and f for D/d=25. The optimize condition was considered for insulated outer wall condition. The Nusselt number variation is taken in primary Y-axis and friction factor in secondary Y-axis. As the D/d ratio

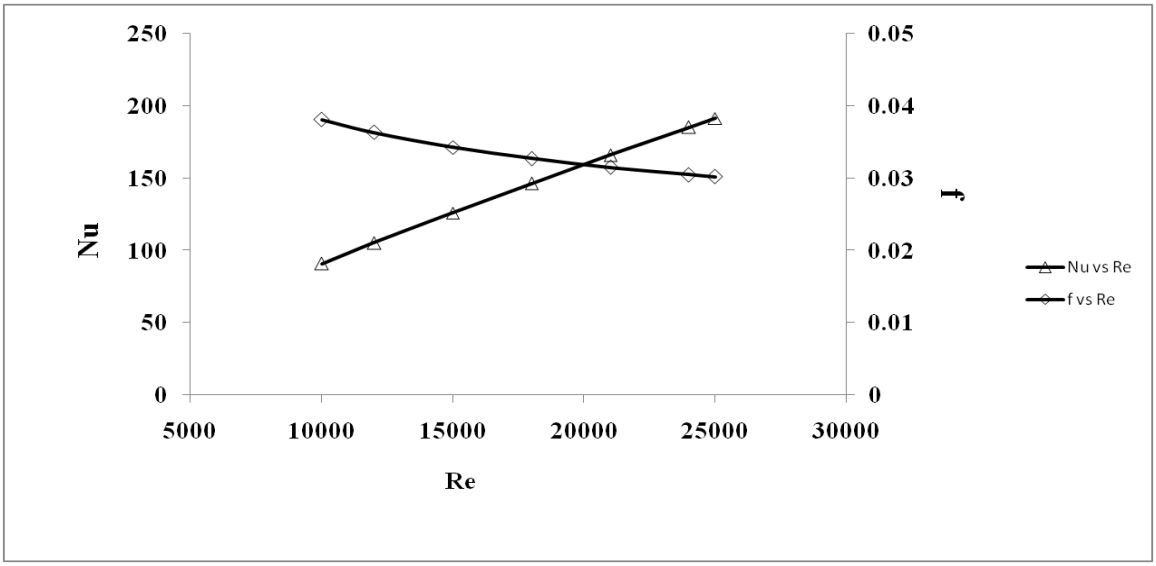

Fig. 5.13 (c) variation of Nu and f with respect to Re for D/d=25

increases the optimizes Reynolds number decreases. For D/d=25 the Reynolds number is 19500. Because with increase in D/d ratio the Reynolds number decreases as shown in Fig.5.8 (a) and Simultaneously the pumping power increases so at smaller Reynolds number, the optimize condition is achieved. Any further increase in Reynolds number Nusselt number increases but the power requirement also increases which will complicate the problem.

Fig .5.13 (d) shows the variation of Re with Nu and also between Re and f for D/d=30. The optimize condition was considered for insulated outer wall condition. The Nusselt number variation is taken in primary Y-axis and friction factor in secondary Y-axis. For D/d=30 the Reynolds number is around 19000.

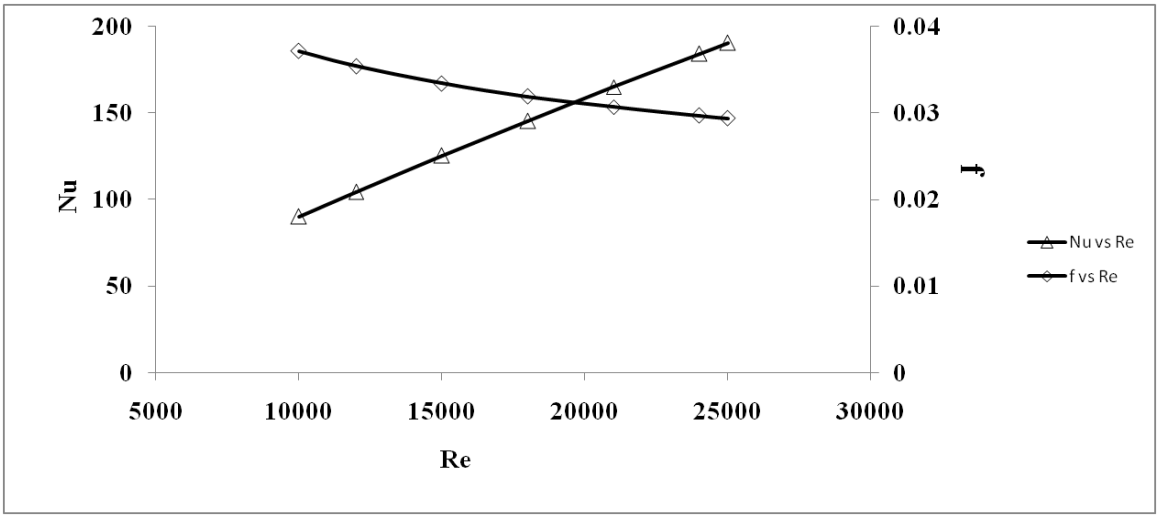

Fig. 5.13 (d) variation of Nu and f with respect to Re for D/d=30

In the Fig. 5.13(a-d) variation between Nu and Re along with f and Re is shown. With increase in Reynolds number, the Darcy friction factor decreases as the pressure drop increases. So Darcy friction factor is the function of pressure drop. But with increase in pressure drop the pumping power increases. So we can assume that with decrease in friction factor pumping power can be increases. For comparison purpose we considered the two non dimensional numbers because it is inconvenient to compare Nusselt number with pumping power. From graph 5.10(a-d) we found that with increase in D/d ratio the Nusselt number decreases and Pumping power increases so the intersection point in Fig. 5.13 (a-d)shifts towards lower Reynolds number.

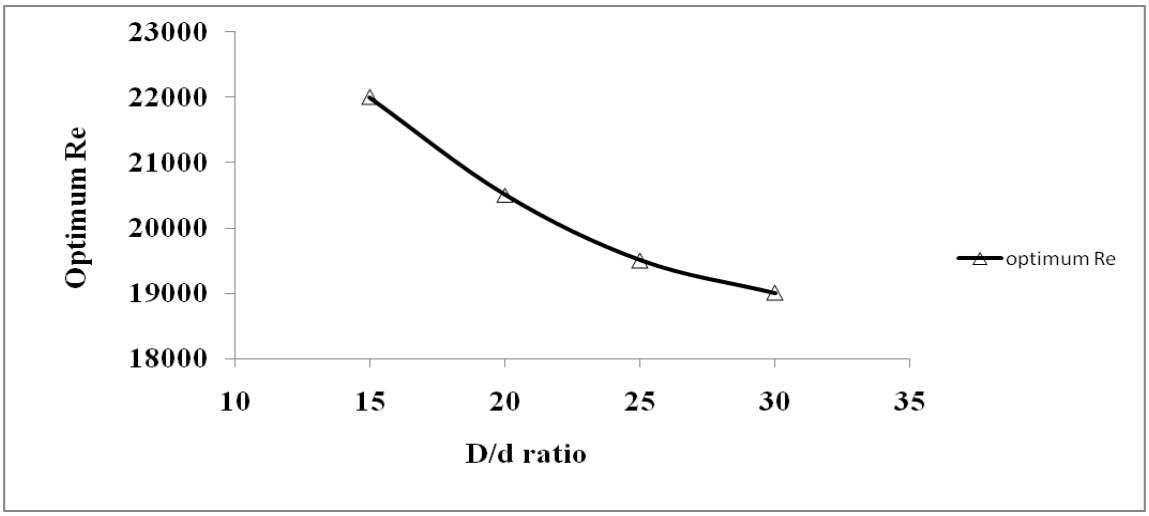

`Fig. 5.14 Optimum Reynolds number with respect to D/d ratio

Fig. 5.14 shows the optimum Reynolds number variation with respect to D/d ratio. As the Nusselt number decreases with D/d ratio and power required increases with D/d ratio, the optimum Reynolds number decreases with increases in D/d ratio.

CHAPTER:-6

CONCLUSIONS AND FUTURESCOPE

Numerical simulation has been carried out for tube in tube helical coil heat exchanger subjected to different boundary conditions. Nusselt number, Darcy friction factor, pumping power required, Log mean temperature difference, pressure drop variation with respect to Reynolds number for different D/d ratio is plotted. In practical application different boundary conditions imposed on the outer wall of exchangers are constant heat flux conditions in power plant boiler, condenser and evaporator etc. insulated outer wall condition in general case of exchanger used in laboratory and educational institutions, and convective heat transfer condition in food, automobile and process industries. Heat transfer behaviors for different boundary conditions are predicted and optimize condition for maximum Nusselt number (Nu) and minimum friction factor (f) was plotted against Reynolds number. Following are the outcome of above numerical study;

- With increase in the Reynolds number, the Nusselt number for the inner tube increase. However, with increases in flow rate turbulence between the fluid element increases which will enhance the mixing of the fluid and ultimately the Nusselt number or the heat transfer rate increases.
- With increases in D/d ratio (inverse of curvature ratio) the Nusselt number will decreases; for a particular value of Reynolds number. Nusselt number has maximum value for D/d=10.
- The outer wall boundary condition does not have any significant effect on the inner Nusselt number, which can be confirmed from the results.
- Friction factor decreases with increase in Reynolds number due to relative roughness of surface, and velocity of flowing fluid.
- Pumping power increases with increase in Reynolds number for all the condition of D/d ratio and for all the boundary conditions. This is due to increase in pressure loss caused

by more turbulent flow. Pumping power is independent of the outer wall boundary conditions.

- Log mean temperature difference increases at a steady rate with increase in Reynolds number.
- As long as the heat transfer is concerned from the hot fluid any boundary condition can be assumed for outer wall of external tube because it does not affect significantly the heat transfer rate.
- From the optimization graph shown between Nu and f with respect to Re; the intersection point shifts toward the lower Reynolds number with increase in D/d ratio. It indicates that lower Reynolds number is required to get maximize condition for higher D/d ratio because the power requirement is more as we move towards higher D/d ratio.
- The optimum Reynolds number decreases with increase in D/d ratio.

Future scope:

The optimization condition presented in this study is by intersection of two graphs. More accurate method should be developed to determine the maximum condition. Along with numerical analysis experimental validation should be required. In this study single phase flow pattern is considered but in future two or multiphase flow may be considered.

REFERENCES

Aly Wael I.A., Numerical study on turbulent heat transfer and pressure drop of nanofluid in coiled tube-in-tube heat exchangers, Energy Conversion and Management, vol.-79 (2014) 304–316.

Eiamsa-ard Smith., Promvonge Pongjet., Enhancement of heat transfer in a tube with regularly-spaced helical tape swirl generators, Solar Energy, vol.-78 (2005) 483–494.

Eiamsa-ard Smith., Promvonge Pongjet., Heat transfer characteristics in a tube fitted with helical screw-tape with/without core-rod inserts, International Communications in Heat and Mass Transfer, vol.-34 (2007) 176–185.

Ferng Y.M., Lin W.C., Chieng C.C., Numerically investigated effects of different Dean number and pitch size on flow and heat transfer characteristics in a helically coil-tube heat exchanger, Applied Thermal Engineering, vol.-36 (2012) 378-385.

Genic Srbislav B., Jacimovic Branislav M., Jaric Marko S., Budimir Nikola J., Dobrnjac Mirko M., Research on the shell-side thermal performances of heat exchangers with helical tube coils, International Journal of Heat and Mass Transfer, vol.-55 (2012) 4295–4300.

Ghorbani Nasser., Taherian Hessam., Gorji Mofid., Mirgolbabaei Hessam., An experimental study of thermal performance of shell-and-coil heat exchangers, International Communications in Heat and Mass Transfer, vol.-37 (2010) 775–781.

Huminic Gabriela., Huminic Angel., Heat transfer characteristics in double tube helical heat exchangers using nanofluids, International Journal of Heat and Mass Transfer, vol.-54 (2011) 4280–4287.

Jahanmir Gh.S., Farhadi F., Twisted bundle heat exchangers performance evaluation by CFD, International Communications in Heat and Mass Transfer, vol.-39 (2012) 1654–1660.

Jamshidi Naghmeh., Farhadi Mousa., Sedighi Kurosh., Ganji Davood Domeiry., Optimization of design parameters for nanofluids flowing inside helical coils, International Communications in Heat and Mass Transfer, vol.-39 (2012) 311–317.

Jamshidi N., Farhadi M., Ganji D.D., Sedighi K., Experimental analysis of heat transfer enhancement in shell and helical tube heat exchangers, Applied Thermal Engineering, vol.-51 (2013) 644-652.

Jayakumar J.S.,Grover R.B., Two phase natural circulation residual heat removal, In Proc. 3rd ISHMT-ASME Heat and Mass Transfer Conference, Kanpur, India. 1997.

Jayakumar J.S., Mahajani S.M., Mandal J.C., Vijayan P.K., Bhoi Rohidas., Experimental and CFD estimation of heat transfer in helically coiled heat exchangers, International journal of Chemical Engineering Research and Design, Vol.-86 (2008):221-232.

Jayakumar J.S, Mahajani S.M., Mandal J.C., Iyer Kannan N., Vijayan P.K., CFD analysis of single-phase flows inside helically coiled tubes, Computers and Chemical Engineering, vol.- 34 (2010) 430–446.

Kharat Rahul., Bhardwaj Nitin., Jha R.S., Development of heat transfer coefficient correlation for concentric helical coil heat exchanger, International Journal of Thermal Sciences, vol.-48 (2009) 2300–2308.

Kumar V., Saini S., Sharma M., Nigam K.D.P., Pressure drop and heat transfer in tube in tube helical heat exchanger, Chemical Engineering Science, vol.-61 (2006): 4403–4416.

Lee Tzong-Shing ., Wu Wu-Chieh., Chuah Yew-Khoy., Wang Sheng-Kai., An improvement of airflow and heat transfer performance of multi-coil condensers by different coil configurations, International journal of refrigeration, vol.-33 (2010) 1370-1376.

Li Yan., Jiang Xiumin., Huang Xiangyong., Jia Jigang., Tong Jianhui., Optimization of high-pressure shell-and-tube heat exchanger for syngas cooling in an IGCC, International Journal of Heat and Mass Transfer, vol.-53 (2010) 4543–4551.

Lu Xing., Du Xueping., Zeng Min., Zhang Sen., Wang Qiuwang., Shell-side thermal-hydraulic performances of multilayer spiral-wound heat exchangers under different wall thermal boundary conditions, Applied Thermal Engineering, Article in press(2014) 1-12.

Naphon Paisarn., Wongwises Somchai., A study of the heat transfer characteristics of a compact spiral coil heat exchanger under wet-surface conditions, Experimental Thermal and Fluid Science, vol.-29 (2005) 511–521.

Paisarn Naphon., Study on the heat transfer and flow characteristics in a spiral-coil tube, International Communications in Heat and Mass Transfer, vol.-38 (2011) 69–74.

Pawar S.S., Sunnapwar Vivek K., Experimental and CFD investigation of convective heat transfer in helically coiled tube heat exchanger, CHERD-1475 (2014) Article in press.

Rennie Timothy J., Raghavan Vijaya G.S., Numerical studies of a double-pipe helical heat exchanger, Applied Thermal Engineering, vol.-26 (2006) 1266–1273.

San Jung-Yang., Hsu Chih-Hsiang., Chen Shih-Hao., Heat transfer characteristics of a helical heat exchanger, Applied Thermal Engineering, vol.-39 (2012) 114-120.

Yang Zhen., Zhao Zhenxing., Liu Yinhe., Chang Yongqiang., Cao Zidong., Convective heat transfer characteristics of high-pressure gas in heat exchanger with membrane helical coils and membrane serpentine tubes, Experimental Thermal and Fluid Science, vol.-35 (2011) 1427–1434.

Zachar A., Investigation of natural convection induced outer side heat transfer rate of coiled-tube heat exchangers, International Journal of Heat and Mass Transfer, vol.-55 (2012) 7892–7901.